MULTIPLE OBJECTIVE OPTIMIZATION OF AN INDUSTRIAL NYLON 6 SEMIBATCH REACTOR USING GENETIC ALGORITHM

A Thesis Submitted

in Partial Fulfillment of the Requirements

for the Degree of

Master of Technology

by

Kishalay Mitra

to the

DEPARTMENT OF CHEMICAL ENGINEERING

INDIAN INSTITUTE OF TECHNOLOGY, KANPUR

April 1997.

CERTIFICATE

This is to certify that the present work entitled, *MULTIPLE OBJECTIVE OPTIMIZATION OF AN INDUSTRIAL NYLON 6 SEMIBATCH REACTOR USING GENETIC ALGORITHM*, by Kishalay Mitra has been carried out under our supervision and that this work has not been submitted elsewhere for a degree.

Dr. Santosh K. Gupta

Professor,

Department of Chemical Engg.

I. I. T, Kanpur

Dr. Kalyanmoy Deb

Assistant Professor,

Department of Mechanical Engg.

I. I. T, Kanpur

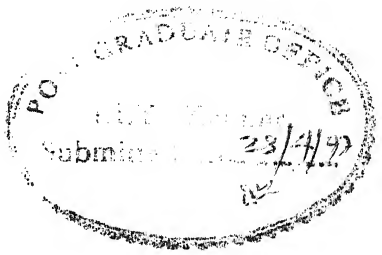

CHE-1997-M-MIT-MUL

ACKNOWLEDGMENT

This thesis (whatever little it does contain) is a result of patience shown and help given by Dr. S. K. Gupta, my guruji and Dr. K. Deb, my Kalyanda. I would like to thank them for giving me almost free hand in expressing myself and doing my work. They were approachable at any time, inspite of their heavy work load. They guided me in all respects of my twenty one month's life at IITK. The regular lab meetings (on Friday) has helped me in getting to see and relish various scenarios of science as well as society (+ve as well as -ve). I shall always be grateful to Dr. G. Biswas, my dearest kaka, for sharing the rare experiences of his life with me. I am also grateful to my TA supervisors and course supervisors who helped me to learn a lot many things as per my capabilities.

It would be amiss not to appreciate the Indian Classical Music Group of IITK (with whom I witnessed the eternal peace of heaven), Cricket Gang of Hall IV and V (with whom I shared my free time occasionally), Indian Music Club Gang of Hall I, II and III (the young and rare music talents of IITK). Special thanks are also due on BIG BOSS (Pallab), SANG (Sanjeev), SOS(Sasanka), NOBU(Nabanita), CHOTA GURUJI (Mankarji), whom I shall miss whenever I shall think of IITK, for being highly pleasant to me. I shall also miss Phal, Dikshitji, Narayan, Kaushik, Shyamal, Munsi, Pabitrada, Tapoda, Tapanda, Manishji, Atulda, Probodhda, Arunda, Berada, Prosenda, Jalda, Sunuda, Shenkuda, Paddy, Sudip, Porel, Ghupu and many others. I would like to give special thanks ('HARIBOOL') to my ISKCON prabhus (Sitanath, Giri, Mahesh, Roopmanohar, KK etc.) for helping me to live in mental peace.

Without 'boudi' (Mrs. Debjani Deb) and 'Kakima' (Mrs. Amarabati Biswas), my life at IITK was not at all lively. I always felt to be at my home at Durgapur, when I went to their place. I can not forget my 'moments' with 'Ronnie' and 'Miku'.

It was always very pleasant to be at house # 518 and sharing 'Pineapple Top Side Bottom' and many other US tastes imported in India. Special thanks to aunti, Ami, Akansha.

In the end, the stay at IITK would have not been so wonderful and carefree but for the love and support of my parents, my elder brother and didi (in Kanpur city). After all, the twenty one months, I think I am leaving IITK as a transformed person. IITK is great place to be. Life is never going to be same again, after leaving IITK.

Thanks,

Kishalay Mitra

CONTENTS

List Of Figures

List of Tables

Nomenclature

a	Specific interfacial area ($m^2\ m^{-3}$)
A	Heat transfer area (m^2)
A_i^o, A_i^c	Frequency factor for $i^{th.}$ reaction in absence (o) and in presence (c) of catalytic effect ($kg\ mol^{-1}\ hr^{-1}$ or $kg^2\ mol^{-2}\ hr^{-1}$)
c , C_S'	Concentration of polymer in solution
conv	Monomer conversion (Eq. 3)
C_i	Caprolactam (i =1) and cyclic dimer (i =2)
$C^v_{p,m}, C^v_{p,w}$	Specific heat of monomer and water in vapor phase ($kJ\ kg^{-1}\ K^{-1}$)
$C^l_{p,mix}$	Specific heat of liquid reaction mixture ($kJ\ kg^{-1}\ K^{-1}$)
d_{jk}	Normalized distance in x space between $j^{th.}$ and $k^{th.}$ points (Eq. 10)
d_s	Diameter of stirrer (m)
D_r	Diameter of the reactor
D_w	Reactor wall thickness (m)
DP	Degree of polymerization of polymer product ($= \mu_n$)
E_i^o, E_i^c	Activation energies for the $i^{th.}$ reaction in absence (o) and in presence (c) of catalytic effect (J/mol)
$F_m^{(i)}$	Fitness function of $i^{th.}$ string
F_i^*	Dummy fitness value of chromosomes in $i^{th.}$ front
$F_{ij}^{*'}$	Shared fitness value of $j^{th.}$ chromosome in $i^{th.}$ front
$\overline{F}_{ij}^{*'}$	Average of the shared fitness values of all the chromosomes in $i^{th.}$ front
F	Mass of liquid in reactor at time t (kg)

h_i	Heat transfer coefficient of liquid (kJ m^{-2} h^{-1} K^{-1})
ΔH_i	Enthalpy of $i^{th.}$ reaction (J/mol)
$\underset{\sim}{I}$	Vector of objective functions, I_m ; m = 1, 2
k	Thermal conductivity of reaction mass (kJ m^{-1} h^{-1} K^{-1})
$k_{l,m}$	Mass transfer coefficient of monomer (m h^{-1})
$k_{l,w}$	Mass transfer coefficient of water (m h^{-1})
k_i	Forward rate constant of $i^{th.}$ reaction
k_i'	Reverse rate constant of $i^{th.}$ reaction
K_i	Equilibrium constant for $i^{th.}$ reaction
m_j	Niche count for $j^{th.}$ point in any front
M_n	Number average molecular weight
M_w	Weight average molecular weight
$[M^v]$	Concentration of caprolactam in vapor phase (mol m^{-3})
n	Number of equations of state variables
n_i	Number of chromosomes in $i^{th.}$ front
$[N^v]$	Concentration of nitrogen in vapor phase (mol m^{-3})
N_{chr}	Total number of binary digits in chromosome = $(N_{ga} + 1) \times N_{str}$
N_g	Generation number
N_{ga}	Number of u_P values which GA generates
N_P	Number of chromosomes in the population
N_{sim}	Number of u_P values after interpolation
N_{str}	Number of binary digits representing each of the control variables
N_{Re}	Reynold's number
N_{Sc}	Schmidt number

N_{Sh}	Sherwood number
O_i	Preferred solutions for $i^{th.}$ case (i = 2, 3, 4 indicating $[W]_0$ = 2.52, 3.45 and 4.43%)
p	Pressure (kPa or atm)
p_c	Crossover probability
p_m	Mutation probability
p_{max}	Maximum pressure (kPa or atm)
P	Total pressure (kPa)
P_i^{sat}	Vapor pressure of component i (kPa)
q	Desired number (approx.) of Pareto points required to be generated
r_i	Net forward rate for $i^{th.}$ reaction (mol kg^{-1} hr^{-1})
R	Gas constant (J/mol-K)
$R_{v,m}$, $R_{v,w}$	Rate of vaporization of monomer and water at time t (mol/hr)
$\underset{\sim k}{\mathbf{s}}^{(i)}$	Substring of N_{str} binary numbers indicating either the value $u_{P,k}^{(i)}$ of or $T_J^{(i)}$
Sh	Sharing function (Eq. 11)
ΔS_i	Entropy change for the i^{th} reaction (J mol^{-1} K^{-1})
S_n	Linear n-mer
t	Time (hr)
t_{fo}	Initially assumed value for t_f (hr.)
t_f	Total reaction time (hr)
T	Temperature (K)
T_J	Jacket fluid temperature (K)
T_r	Reference temperature (K)
TOL	Tolerance in D02EJF code of NAG library

N_{Sh}	Sherwood number
O_i	Preferred solutions for $i^{th.}$ case (i = 2, 3, 4 indicating $[W]_0$ = 2.52, 3.45 and 4.43%)
p	Pressure (kPa or atm)
p_c	Crossover probability
p_m	Mutation probability
p_{max}	Maximum pressure (kPa or atm)
P	Total pressure (kPa)
P_i^{sat}	Vapor pressure of component i (kPa)
q	Desired number (approx.) of Pareto points required to be generated
r_i	Net forward rate for $i^{th.}$ reaction (mol kg^{-1} hr^{-1})
R	Gas constant (J/mol-K)
$R_{v,m}$, $R_{v,w}$	Rate of vaporization of monomer and water at time t (mol/hr)
$\underset{\sim k}{s^{(i)}}$	Substring of N_{str} binary numbers indicating either the value $u_{P,k}^{(i)}$ of or $T_J^{(i)}$
Sh	Sharing function (Eq. 11)
ΔS_i	Entropy change for the i^{th} reaction (J mol^{-1} K^{-1})
S_n	Linear n-mer
t	Time (hr)
t_{fo}	Initially assumed value for t_f (hr.)
t_f	Total reaction time (hr)
T	Temperature (K)
T_J	Jacket fluid temperature (K)
T_r	Reference temperature (K)
TOL	Tolerance in D02EJF code of NAG library

T_J^{min}, T_J^{max}	Lower and upper bounds on jacket fluid temperature
$\underset{\sim}{\mathbf{u}}$	Vector of control variables, $u_{P,k}^{(i)}$
$u_{P,k}^{(i)}$	Value of control variable at the end of $k^{th.}$ time interval in the $i^{th.}$ chromosome
$u_{P,k}^{min}, u_{P,k}^{max}$	Lower and upper bounds on control variable at the end of $k^{th.}$ time interval
U	Overall heat transfer coefficient (kJ h^{-1} m^{-2} K^{-1})
U_i	Utopia for $i^{th.}$ case (i = 2, 3, 4indicating $[W]_0$ = 2.52, 3.45 and 4.43%)
V_g	Volume of vapor space (m^3)
V_T	Rate of vapor release from reactor (mol/hr)
w_1, w_2	Weightage factors
W	Water
$[W^v]$	Concentration of water in vapor (mol m^{-3})
$\underset{\sim}{\mathbf{x}}$	Vector of state variables, x_i

Greek Letters

α	Exponent controlling the sharing effect
γ_m	Activity coefficient of monomer
γ_w	Activity coefficient of water
ζ_i	Total mol of m (i = 1), w (i = 2) or both (i =3) vaporized to time t (mol)
η	Viscosity of liquid mixture (Pa s or poise; 1 poise = 10^{-1} Pa s)
$[\eta]$	Intrinsic viscosity of ε-caprolactam-nylon 6 mixture (100 kg mixture / kg polymer)

θ	Dimensionless temperature
λ_m, λ_w	Latent heats of vaporization of monomer, water (J/mol)
μ_k	k^{th} moment of the chain length distribution (k = 0,1,2, . . .) ; $\mu_k \equiv \sum_{n=1}^{\infty} n^k [S_n]$ (mol/kg)
μ_n	Number average chain length $\left(\equiv \frac{\mu_1}{\mu_0} \right)$
Π	Dimensionless pressure (Eq. 1(a))
ρ	Density of liquid reaction mixture (kg m^{-3})
τ	Dimensionless time (Eq. 1(b))
σ_{share}	Maximum normalized distance in x space between any two points (Eq. 12)

Subscripts/Superscripts

b	bubble
d	Desired value
f	Final (value for the product)
f	film
J	jacket
m	monomer
max	maximum value
o	Feed conditions
ref	Reference (value used in industrial reactor currently)
sat	saturation value

t_f	Value at $t = t_f$
w	water

Symbols

[ ]	Concentrations (mol / kg mixture)

Abstract

The Nondominated Sorting Genetic Algorithm (NSGA) is adapted and used to obtain multiobjective Pareto optimal solutions for three grades of nylon 6 being produced in an industrial semibatch reactor. The total reaction time and the concentration of undesirable cyclic dimer in the product, are taken as two individual objectives for minimization, while simultaneously requiring the attainment of design values of the final monomer conversion and for the number average chain length. Substantial improvements in the operation of the nylon 6 reactor are indicated by this study. The technique used is very general in nature and can be used for multiobjective optimization of other reactors. Good mathematical models accounting for all the physico-chemical aspects operative in a reactor (and which have been preferably tested on industrial data) are a prerequisite for such optimization studies.

Chapter 1

Introduction

Most real world decision making design problems require simultaneous optimization of multiple objectives depending upon the nature of the system. Multiple objective optimization problems are conceptually different from single objective optimization problems. Single objective optimization problems always find the global optimal solution (maximum or minimum depending upon the requirement of a particular system). In case of multiobjective optimization, a *set* of solutions is obtained which are not necessarily the global best solutions if any of the objectives is considered individually, but are relatively better feasible optimal solutions depending upon the requirements of the designer if all the objectives are considered simultaneously. This set of solutions is called the Pareto-optimal or nondominated solutions. In this study, multiobjective optimization of an industrial nylon 6 reactor is being carried out, and Pareto-sets are generated. These help to channelize the thinking of a decision maker in identifying suitable operating or design conditions.

A number of studies have been reported on the optimal temperature and initiator or monomer addition histories (or profiles) for free radical and step-growth polymerizations

in batch, semibatch, or plug-flow reactors. These have been reviewed by Farber.[1] In most of the studies discussed in the review a single objective function is used which is a weighted average of a few individual objectives as, for example, (a) concentration of unreacted monomer in the product, (b) concentration of undesirable side products, (c) reaction time, (d) deviation of the number average chain length (μ_n) and/or polydispersity index (PDI) from the desired values, etc. This type of scalar optimization approach suffers from the drawback that the results are highly sensitive to the values of the weightage factors used. In addition, there is a chance of loosing some optimal solutions.[2,3] In vector or multiobjective optimization, the objective function, $\underset{\sim}{I}$, is a vector, comprising of a few individual objective functions, I_i. The optimal solutions obtained using this approach help a designer to make better decisions. Since most optimization problems in polymer reaction engineering deal with different interesting and often conflicting objectives, multiobjective function optimization offers tremendous prospects for use in the optimal design and operation of these reactors. Some studies[4-9] have already been reported on the optimization of polymerization reactors using this approach, but none of these involves industrial reactors. In this work, we have optimized the operation of an *industrial* nylon 6 reactor. This reactor has been simulated by our group earlier,[10-12] and a satisfactory mathematical model is already available, which can be used confidently for optimization purposes.

Most of the earlier studies on the optimization of polymerization reactors involving single as well as multiple objective functions, use Pontryagin's minimum principle[13,14] or some pattern search techniques to arrive at optimal solutions. These traditional techniques usually require a good initial guess of the optimal solution, i.e., of the control variable histories. It is well known that Pontryagin's technique is particularly sensitive to the choice

of the initial guess. In fact, for complex, real-life problems (e.g., for methyl methacrylate polymerization, as well as for nylon 6 polymerization,[16-18] the 'window' in which the initial guess of the control variable must lie, is extremely narrow, and one can easily get into problems of lack of convergence. One often has to generate solutions of similar or easier problems before one gets an idea of good initial guesses.These techniques are, thus, not suitable for on-line applications. A new and extremely powerful search technique based on the mechanics of natural genetics and natural selection, called genetic algorithm (GA) is becoming popular in the literature. This technique does not require initial guesses of the control variable. This is a very robust technique and can be made to converge to the global optimum even in the presence of several local optima. Details of GA as well as of its several adaptations and extensions, are available in several books.[19-21] A computer code (SGA - Simple Genetic Algorithm) which uses the basic algorithm is available now,[21] and this can be used as such or as a part of any larger code using any adaptation of this algorithm. In this work, however, we have used the nondominated sorting genetic algorithm (NSGA[22]) which is quite similar to the simple genetic algorithm (SGA) except for some differences in the working principle of the selection operator. Details of this adaptation are discussed later.

Pareto sets for the industrial nylon 6 reactor are obtained using this technique. It is found that significant improvements (reduction in reaction time, reduction in the concentration of undesired side product) are indicated over the current operation of the reactor. We understand that some changes in the operating variables have been made in industry along the directions suggested by our studies, and considerable improvements have, indeed, been achieved.

Chapter 2

Formulation

The industrial reactor[10-12] studied herein is shown schematically in Fig. 1. It is a jacketed vessel with a low speed anchor or ribbon agitator used for mixing the highly viscous reaction mass. The reaction mass (ε-caprolactam, C_1, water, W, and other inert additives like TiO_2, etc.) is heated by condensing vapor in a jacket in which the fluid is at temperature, T_J, (a constant value independent of time). As the polymerization takes place the temperature, T, inside the reactor goes above 220°C and vaporization of ε-caprolactam and water occurs, resulting in a build-up of the pressure, p, in the region above the liquid reaction mass. The pressure inside the reactor, p(t), is maintained such as to conform to a desired history by manipulation of a control valve. The latter allows the vapor mixture of nitrogen (inert, used initially above the liquid), monomer and water to pass through to a condenser at a prescribed rate, V_T (mol of mixture/hr). The pressure histories used currently (all current values are referred to as 'reference' conditions denoted by ref.) for three different industrial runs producing different grades of nylon 6 (using different initial concentrations of water, $[W]_0$), are shown in Fig. 2 (curves marked "ref."). In this diagram, the pressure and the time, t, have been nondimensionalized using

$$\Pi \equiv (p - p_0) / (p_{max,ref} - p_0) \qquad (a)$$

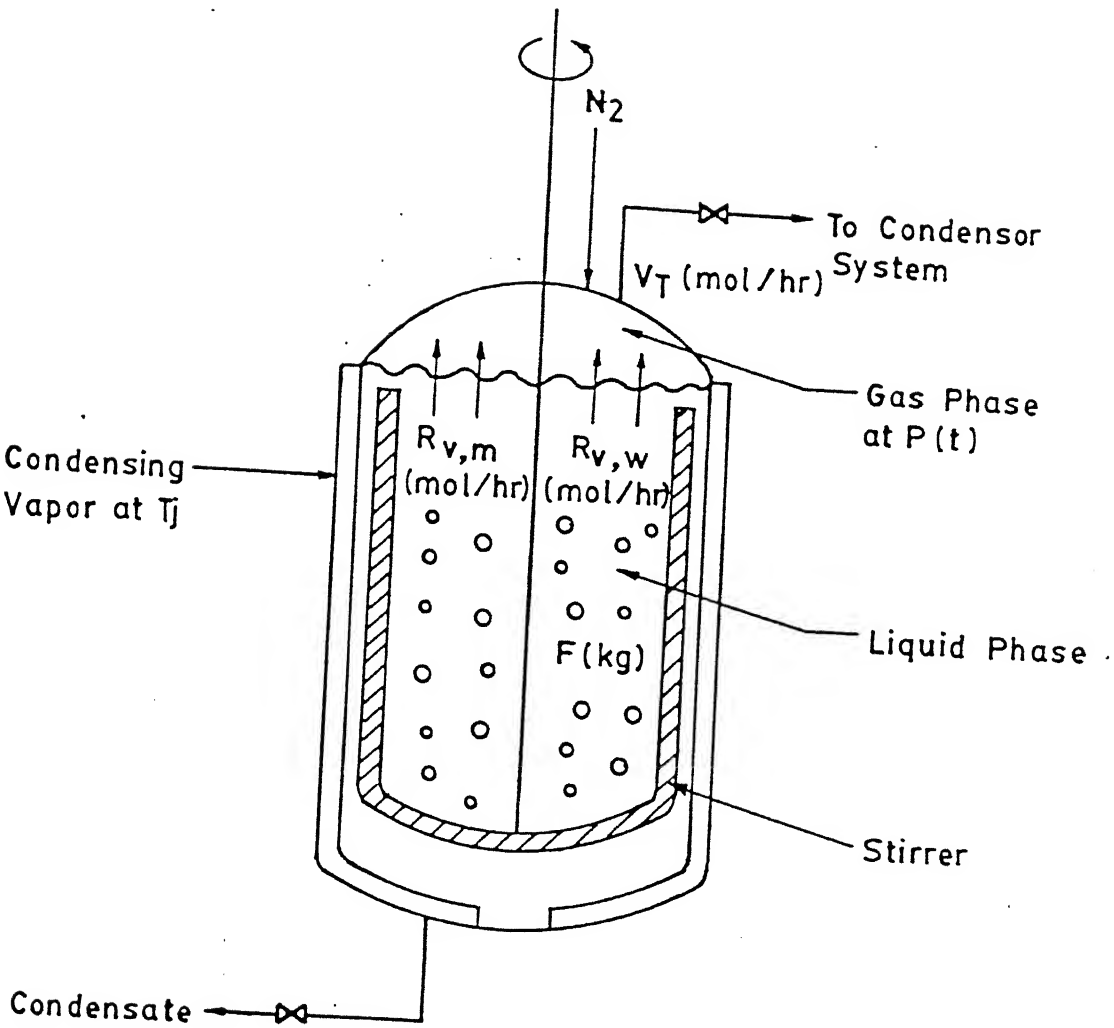

Fig. 1 : Schematic diagram of the industrial semibatch nylon 6 reactor.

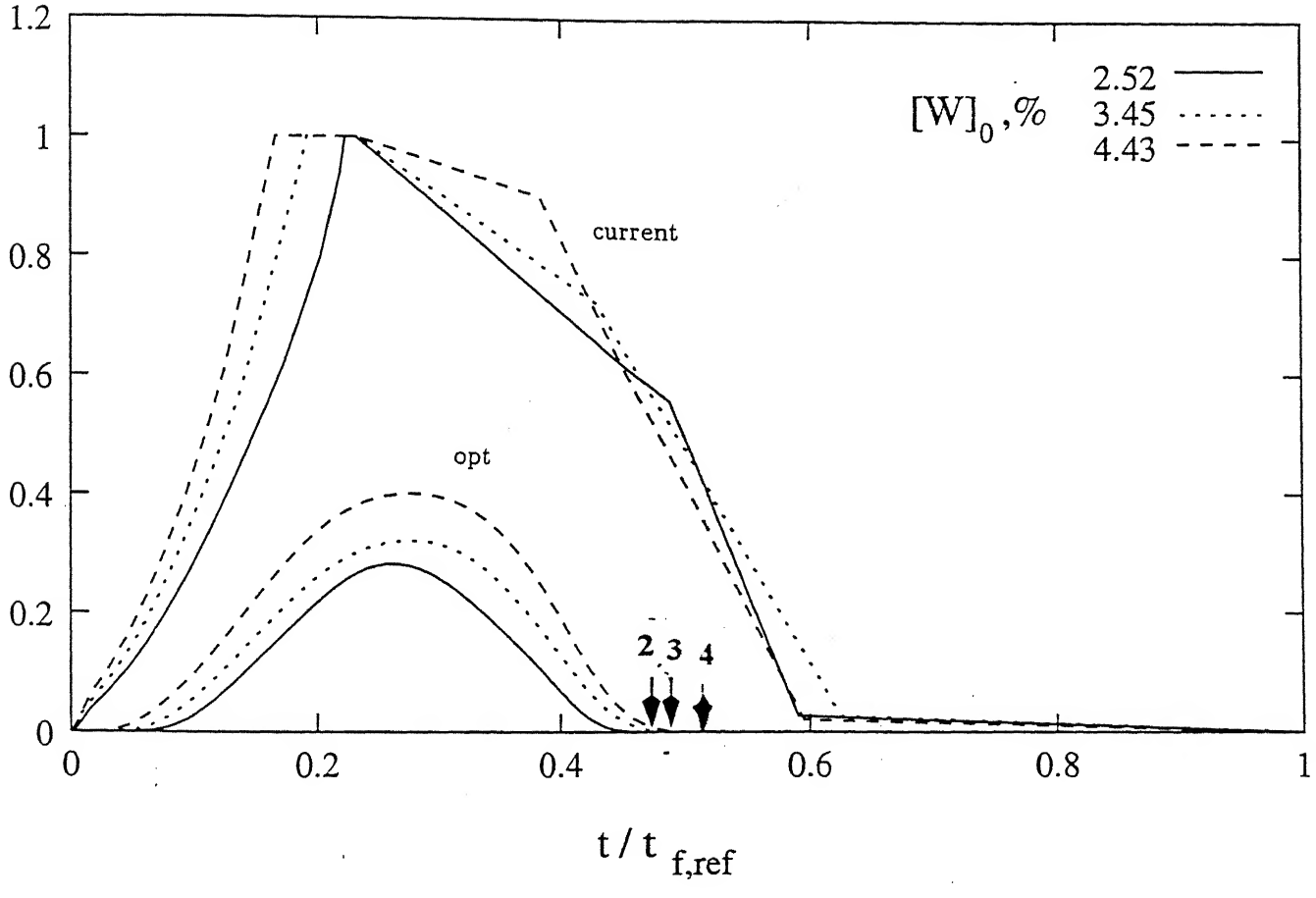

Fig. 2 : Dimensionless pressure histories used currently to produce three grades of nylon 6, using different values of $[W]_0$.[12] Optimal histories corresponding to points, O_i , in the Pareto optimal solutions also shown. Arrows indicate the values of t_f / $t_{f,ref}$ for the three $[W]_o$.

$$\tau \equiv t / t_{f,ref} \qquad \text{(b)} \quad (1)$$

Details of the model used (see Appendix 1), operating conditions, and results of simulation, are available in Ref. 12. Five model parameters were 'tuned' using only one set (one value of $[W]_0$) of industrial data, and it was found that this tuned model gave results which compared satisfactorily with industrial data for the other two grades of polymer without requiring any retuning of the model-parameters. This indicated that all the physico-chemical phenomena playing an important role in the reactor, are being correctly modeled. The model[1,2] is used without any change for multifunctional optimization.

The kinetic scheme for nylon 6 polymerization is given in Table 1.[23-25] This scheme incorporates three important reactions, viz., ring opening, polycondensation and polyaddition, as well as two side reactions involving the cyclic dimer, C_2. Because of the non-availability of precise information about the rates of reactions involving the higher cyclic oligomers, C_3, C_4,..., these have not been incorporated in Table 1. Since the cyclic dimer constitutes a major share of the total cyclic oligomers in the reaction mass, this simplification of the kinetic scheme is justified. The 'state' of the reactor can be well described by a set of fifteen state variables, $\underset{\sim}{\mathbf{x}}\{\equiv[x_1, x_2, \ldots, x_{15}]^T\}$. Equations for these can easily be written using mass and energy balances, and by obtaining moments of the polymer chain-length distribution, and are given in Ref. 12 as well as in Appendix 1. In general, the state variable equations can be written in the form:

$$\frac{dx_i}{dt} = f_i(\underset{\sim}{\mathbf{x}}, \underset{\sim}{\mathbf{u}}) \; ; \; i = 1, 2, \ldots, 15 \qquad (2)$$

where $\underset{\sim}{\mathbf{x}}$ and $\underset{\sim}{\mathbf{u}}$ are the vectors of the state and the control variables.

1. Ring Opening

$$C_1 + W \underset{k_1' = \frac{k_1}{K_1}}{\overset{k_1}{\rightleftharpoons}} S_1$$

2. Polycondensation

$$S_n + S_m \underset{k_2' = \frac{k_2}{K_2}}{\overset{k_2}{\rightleftharpoons}} S_{m-n} + W; n, m = 1,2,...$$

3. Polyaddition

$$S_n + C_1 \underset{k_3' = \frac{k_3}{K_3}}{\overset{k_3}{\rightleftharpoons}} S_{n+1}; n = 1,2,...$$

4. Ring Opening Of Cyclic Dimer

$$C_2 + W \underset{k_4' = \frac{k_4}{K_4}}{\overset{k_4}{\rightleftharpoons}} S_2$$

5. Polyaddition Of Cyclic Dimer

$$S_n + C_2 \underset{k_5' = \frac{k_5}{K_5}}{\overset{k_5}{\rightleftharpoons}} S_{n+2}; n = 1,2,...$$

contd.

$$k_i = A_i^0 \exp\left(-E_i^0/RT\right) + A_i^c \exp\left(-E_i^c/RT\right)\sum_{n=1}^{\infty}\left([S_n]\right) = k_i^0 + k_i^c \sum_{n=1}^{\infty}\left[S_n\right]$$

$$K_i = \exp\left[\left(\Delta S_i - \Delta H_i/T\right)/R\right], i = 1,2,\ldots,5$$

i	A_i^0 (kg/mol-h)	E_i^0 (cal/mol)	A_i^c (kg^2/ mol^2-h)	E_i^c (cal/mol)	ΔH_i (cal/mol)	ΔS_i (cal/ mol-K)
1	5.9874 $\times 10^5$	1.9880 $\times 10^4$	4.3075 $\times 10^7$	1.8806 $\times 10^4$	+1.9180 $\times 10^5$	-7.88460
2	1.8942 $\times 10^{10}$	2.3271 $\times 10^4$	1.2114 $\times 10^{10}$	2.0670 $\times 10^4$	-5.9458 $\times 10^5$	−0.94374
3	2.8558 $\times 10^9$	2.2845 $\times 10^4$	1.6377 $\times 10^{10}$	2.0107 $\times 10^4$	-4.0438 $\times 10^5$	-6.94570
4	8.5778 $\times 10^{11}$	4.2000 $\times 10^4$	2.3307 $\times 10^{12}$	3.7400 $\times 10^4$	-9.6000 $\times 10^5$	-14.5200
5	2.5701 $\times 10^8$	2.1300 $\times 10^4$	3.0110 $\times 10^9$	2.0400 $\times 10^4$	-3.1691 $\times 10^5$	−0.58265

Table 1: Kinetic Scheme For Nylon 6 Polymerization [23-25] and corresponding rate parameters.

The ODEs (ordinary differential equations) in Eq. 2 can be integrated using the D02EJF subroutine of the NAG library for any given $\underline{u}(t)$ and initial conditions. This subroutine uses Gear's technique for integrating sets of stiff ODEs[26]. The presence of some discontinuities and the stiffness of the ODEs makes it difficult to use a constant error tolerance (TOL) in the computer code, D02EJF. Provision was made in the algorithm for self-adjustment of the error tolerance between 10^{-4} and 10^{-12}. If the set of ODEs cannot be integrated for a certain value of TOL, the simulation package decreases the value of this parameter by a factor of 10 and integrates the set of differential equations again from the previous value of t (for which converged results have been obtained). This is attempted between upper and lower limits of TOL. This simulation package is combined with the NSGA[22] optimization code for performing multifunctional optimization.

Two objective functions (both to be minimized) are considered in this study. The first involves the nondimensional reaction time, $t_f/t_{f,ref}$. The total reaction time, t_f, is determined as the time at which the monomer conversion, conv, reaches the desired value, $conv_{f,ref}$ (the value obtained in industry presently) as well as the degree of polymerization, $\mu_{n,f}$, reaches the desired value, $\mu_{n,ref}$. The monomer conversion in a semibatch reactor at any time, t, is defined as

$$conv \equiv 1 - \frac{F[C_1] + \zeta_1}{F_0[C_1]_0} \qquad (3)$$

where F and $[C_1]$ represent the total mass of the liquid reaction mixture and the concentration (mol/kg) of the monomer at any time, respectively, and subscript, 0, represents the initial values. ζ_1 is the (cumulative) amount (mol) of monomer that has vaporized until time t.

The first of the above requirements (on conv) ensures that the monomer recycling load remains the same as at present, while the second requirement (on μ_n) ensures that the

physical properties of the product polymer (determined by μ_n primarily) are the same as those of the polymer currently produced. One may or may not be able to satisfy both of these two requirements at $t = t_f$ simultaneously. To account for this, the integration of the model equations (Eq. 2) is terminated at the point where $conv = conv_{f,ref}$. This denotes the point t_f. The value, $\mu_{n,f}$, of μ_n at this point is incorporated in the first objective function, I_1, in the form of a penalty function with weightage factor, w_1

$$I_1 = t_f / t_{f,ref} + w_1(1 - \mu_{n,f} / \mu_{n,ref})^2 \qquad (4)$$

Minimization of I_1 leads to an increase in the production capacity of the industrial plant (through $t_f/t_{f,ref}$), while simultaneously giving preference to solutions satisfying the requirement, $\mu_{n,f} = \mu_{n,ref}$ (alongwith $conv_f = conv_{f,ref}$).

The second objective function, I_2, involves the nondimensional concentration, $[C_2]_f/[C_2]_{f,ref}$, of the undesirable cyclic dimer in the polymer produced. These cyclics cause problems in polymer processing[23-25] and are removed by hot water extraction, which is an energy consuming process. Minimization of $[C_2]_f/[C_2]_{f,ref}$, thus, leads to improvement of the product quality, as well as reduces extraction costs downstream. The penalty on the violation of $\mu_{n,f} = \mu_{n,ref}$ is also included in I_2 with weightage factor, w_2. Thus,

$$I_2 = [C_2]_f / [C_2]_{f,ref} + w_2(1 - \mu_{n,f} / \mu_{n,ref})^2 \qquad (5)$$

The use of penalty functions involving $\mu_{n,f}$ in both the objective functions, and the use of the condition, $conv_f = conv_{f,ref}$, to stop the integration of the state variable equations, ensures that we obtain optimal solutions where $t_f/t_{f,ref}$ and $[C_2]_f/[C_2]_{f,ref}$ are minimized, while ensuring $conv_f = conv_{f,ref}$ as well as $\mu_{n,f} = \mu_{n,ref}$.

The two objectives (Eqs. 4 and 5) are conflicting in nature and, therefore, provide an excellent opportunity for carrying out multifunctional optimization. In the industrial reactor, the vapor release rate *history*, $V_T(t)$, and the jacket fluid temperature, T_J (a

constant *value*), are used as the control (or optimizing) variables. These two constitute our control vector, $\underset{\sim}{\mathbf{u}}$. Thus, our optimization problem can be written in mathematical form, as

$$\underset{T_J, V_T(t)}{\text{Min}} \; \underset{\sim}{\mathbf{I}} \equiv \left[I_1 , I_2 \right]^T \qquad \text{(a)}$$

where

$$I_1^{(i)} = t_f^{(i)} / t_{f,ref} + w_1 (1 - \mu_{n,f}^{(i)} / \mu_{n,ref})^2 \qquad \text{(b)}$$

$$I_2^{(i)} = [C_2]_f^{(i)} / [C_2]_{f,ref} + w_2 (1 - \mu_{n,f}^{(i)} / \mu_{n,ref})^2 ; \; i = 1, 2, \ldots, N_P \qquad \text{(c)}$$

$$\text{conv}_f = \text{conv}_{f,ref} \qquad \text{(d)}$$

mass and energy balance equations (e)

any additional physical limits on the control variables (f) (6)

The solution of the multiobjective optimization problem described in Eq. 6 is obtained using the nondominated sorting genetic algorithm (NSGA)[22] *adapted* in this study so as to apply for control variables which are continuous functions of time, t. Details of this adapted NSGA are described below, and the associated flowchart is given in Table 2. The numbers in the discussion below refer to the numbered boxes in Table 2.

4. At generation number, N_g=0, a population having N_p chromosomes (members) is generated. Each chromosome in this population carries the information of one digitized control variable *history* [set of vapor release rate, $V_T(t)$, values] and one control variable *value* (a single value of the jacket fluid temperature, T_J). We discretize our first control variable history, $V_T(t)$, in terms of N_{ga} equispaced points in $0 \le t \le t_{f0}$ (t_{f0}, an initial estimate of t_f , is to be supplied). The second control variable, T_J , is appended in any chromosome as an additional [$(N_{ga}+1)^{th}$] point. Thus, each of the N_p chromosomes (called strings) comprises of a sequence of (N_{ga} + 1) numbers (called substrings). Each of these substrings, in turn, comprises of a set of N_{str} binary numbers (0 or 1). Each chromosome,

1. Input data :

N_P, N_{str}, N_{ga}, N_{sim}, p_m, p_c, q,α,

$t_{f0}, u_{P,k}^{min}, u_{P,k}^{max} (k = 1,2,\ldots,N_{ga}), T_J^{min}, T_J^{max}, N_{g,max}$

$N_{chr} = (N_{ga} + 1) \times N_{str}$

2. Initialize generation number :

$N_g = 0$

3. Initialize random number generator.

4. Create N_P random binary chromosomes, each of length N_{chr} having N_{str} binaries for each of the N_{ga} points representing $u_P(t)$ history and N_{str} binaries (bits) representing the single value of T_J.

$$\underset{\sim}{s}^{(i)} \equiv \left[\underset{\sim 1}{s}^{(i)}, \underset{\sim 2}{s}^{(i)}, \ldots, \underset{\sim N_{ga}}{s}^{(i)}, \underset{\sim N_{ga}+1}{s}^{(i)} \right]$$

where $\underset{\sim k}{s}^{(i)} \equiv \left[b_{1,k}^{(i)}, b_{2,k}^{(i)}, \ldots, b_{N_{str},k}^{(i)} \right]$

where $b_{j,k}^{(i)} \in \{0,1\}$

$i = 1, 2, \ldots, N_P$; $j = 1, 2, \ldots, N_{str}$; $k = 1, 2, \ldots, N_{ga} + 1$

5. Decode and adaptively map each chromosome to give a digitized $u_P(t)$ history with N_{ga} real values and a real value of T_J, using

$$u_{P,k}^{(i)} = u_{P,k}^{(min)} + \frac{u_{P,k}^{(max)} - u_{P,k}^{(min)}}{2^{N_{str}} - 1} \times \begin{pmatrix} \text{decoded value} \\ \text{of} \quad s_k^{(i)} \end{pmatrix}$$

$$T_J^{(i)} = T_J^{(min)} + \frac{T_J^{(max)} - T_J^{(min)}}{2^{N_{str}} - 1} \times \begin{pmatrix} \text{decoded value} \\ \text{of} \quad s_{N_{ga}+1}^{(i)} \end{pmatrix};$$

$k = 1, 2, \ldots, N_{ga}$; $i = 1, 2, \ldots, N_P$

6. For each chromosome, use Hermite interpolation of the N_{ga} discrete values $u_{P,k}^{(i)}$, of $u_P(t)$ to get a continuous $u_P(t)$ history. Obtain N_{sim} ($>> N_{ga}$) equispaced intermediate real values, $[U_{P,l}^{(i)}]; l = 1,2,\ldots, N_{sim}$, describing the $u_P(t)$ history:

$$\left[\underset{\sim P}{\mathbf{U}}^{(i)}\right] = \left[U_{P,1}^{(i)}, U_{P,2}^{(i)}, \ldots U_{P,N_{sim}}^{(i)} \right]$$

7. For each chromosome representing a $U_P^{(i)}(t)$ history and a value of $T_J^{(i)}$, solve the model equations (Eqn. 2 or Appendix 1) using Gear's algorithm with stopping condition as $conv_i = conv_{i,ref}$. Record $I_1^{(i)}$ and $I_2^{(i)}$ (Eqn. 4). Compute the fitness values, $F_1^{(i)}$ and $F_2^{(i)}$, as $F_m^{(i)} = 1/\left(1 + I_m^{(i)}\right)$; for all $i = 1, 2, \ldots, N_P$ and $m = 1, 2$. Identify all feasible solutions.

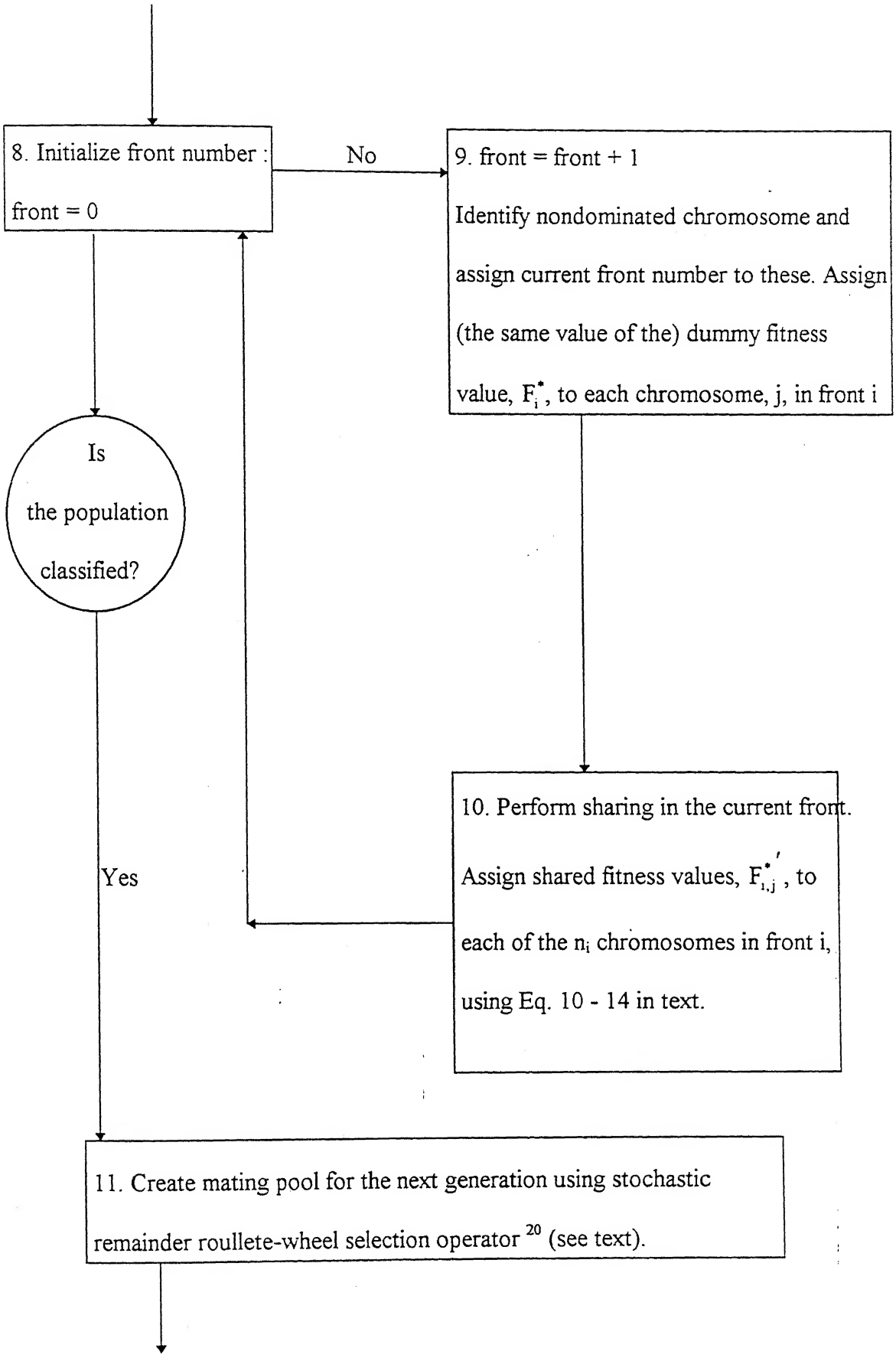
8. Initialize front number :
front = 0
No
9. front = front + 1
Identify nondominated chromosome and assign current front number to these. Assign (the same value of the) dummy fitness value, F_i^*, to each chromosome, j, in front i
Is the population classified?
Yes
10. Perform sharing in the current front. Assign shared fitness values, $F_{i,j}^{*\prime}$, to each of the n_i chromosomes in front i, using Eq. 10 - 14 in text.
11. Create mating pool for the next generation using stochastic remainder roullete-wheel selection operator [20] (see text).

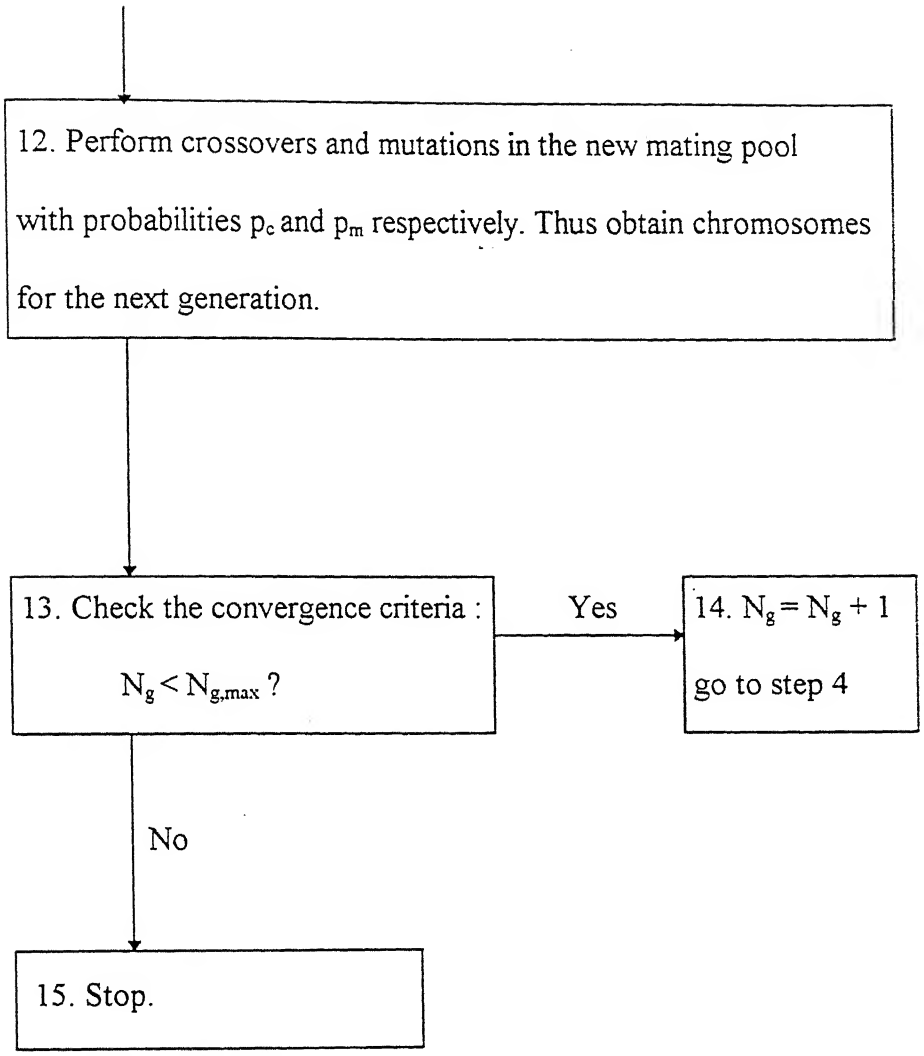

Table 2: Flowchart Describing the Adapted NSGA Used in This Study.

therefore, has $N_{chr} = \left(N_{ga} + 1\right) \times N_{str}$ binary digits, $b_{j,k}^{(i)}$ (see box No. 4 of Table 2). The N_{chr} individual binaries in each of the N_p chromosomes, are generated using a random number generation subroutine.[9,20,21]

5. The complete binary string (sequence of N_{chr} binaries) of the i^{th} chromosome, when decoded into real numbers, $u_{p,k}^{(i)}$ or $T_J^{(i)}$ and interpolated (mapped) between the upper ($u \leq u^{max}$) and lower ($u \geq u^{min}$) bounds of the control variables $\underset{\sim}{\mathbf{u}}$, gives a digitized $u_P^{(i)}$-history (a set of N_{ga} real values), $[u_{P,1}^{(i)}, u_{P,2}^{(i)}, \ldots, u_{P,N_{ga}}^{(i)}]$, representing a $V_T(t)$ history as well as a value, $T_J^{(i)}$, representing a single value of the jacket fluid temperature T_J, corresponding to that chromosome. Thus, there is a set of N_p chromosomes, each representing a digitized $u_P(t)\left[\equiv V_T(t)\right]$ history and a value of T_J, each appropriately coded, in the form of a string of N_{chr} binaries. The minimum difference between the digitized values of the control variable (at any value, t_k) of two different chromosomes is $(u_{p,k}^{max} - u_{p,k}^{min}) / (2^{N_{str}} - 1)$. This is the accuracy to which any particular u_P can be determined for different members of the population in a particular generation..

6. The decoded and adaptively mapped, discretized values, $u_{p,k}^{(i)}$, are curve-fitted piece-wise (splines) to obtain a continuous *function*, $U_P^{(i)}(t)$. A piece-wise cubic Hermite subroutine (E01BFF from the NAG library) is used to do this. This continuous function is again digitized to give N_{sim} ($\geq N_{ga}$) values of the control variable, $[U_{P,l}^{(i)}; l = 1, 2, \ldots, N_{sim}]$.

7. These more closely spaced, discretized values of $U_P^{(i)}(t)$ and the value of $T_J^{(i)}$ are fed to the simulation package, D02EJF (of NAG library) which integrates the state variable equations (Eq. 2 or Appendix 1) starting with the given initial conditions[12] and terminating at the stopping condition, $conv_f = conv_{f,ref}$. The simulation program stores the values of each of the state variables, $\underset{\sim}{\mathbf{x}}^{(i)}(j)$, at every N_{sim} intermediate values of t, such that there are

sets of $\underset{\sim}{x}$ values until $conv_f = conv_{f,ref}$. These detailed histories could be printed out later for the optimal solutions. The values of the two objective functions I_1 and I_2 [at the final reaction time $t = t_f$, see Eqs. 6 (b) and (c)] are computed. One additional point needs to be emphasized. The computer codes involving GA usually *maximize* a fitness function, $F_m^{(i)}$, rather than minimize objective functions, $I_m^{(i)}$, m = 1, 2. Hence we define fitness functions to convert the minimization problem to an equivalent maximization problem as follows:

$$F_1^{(i)} \equiv 1/\left(1+I_1^{(i)}\right)$$
$$F_2^{(i)} \equiv 1/\left(1+I_2^{(i)}\right) \qquad (7)$$

It may be added that the technique described till this stage is quite similar to that[9] developed for the optimization of MMA polymerization. All the feasible points are identified (for plotting) at this stage. The feasible points or chromosomes are those for which $conv_f = conv_{f,ref} + 0.009$ and $(1- \mu_n/\mu_{n,ref}) = \pm 0.009$. The satisfaction of the latter requirement means that the penalty value in Eq. 4 and 5 are negligible.

9. A chromosome, i_1, is said to be dominated by another chromosome, i_2, (for the present problem of minimization of $\underset{\sim}{I}$ or maximization of $\underset{\sim}{F}$), if

$$F_1^{(i_1)} < F_1^{(i_2)} \qquad \text{(a)}$$

as well as

$$F_2^{(i_1)} < F_2^{(i_2)} \qquad \text{(b)}$$

then

i_1 is dominated by i_2 (c) (8)

For example, in Fig. 3 point 3 is dominated by point 5. We test each of the N_P chromosomes in the population against all others to sort out *all* dominated chromosomes. As soon as a chromosome is found to be dominated, if is not checked for dominance with

any other chromosome in the population. When all chromosomes have been checked for dominance, and all dominated chromosomes have been identified, the rest of the chromosomes are given a front number, FRONT=1. These chromosomes having FRONT=1, are called nondominated chromosomes. In Fig. 3, points 4, 5, 6 will constitute the chromosomes assigned FRONT=1. All nondominated chromosomes are then assigned a *dummy* fitness value, F_1^* equal to N_P. Thereafter these *dummy* fitness values are modified according to the *sharing* procedure described in item 10 below, to assign a *shared fitness* value. Sharing is done to maintain diversity in the nondominated chromosomes.[27] In order to identify chromosomes for other fronts, we temporarily discard all nondominated chromosomes. The ***remaining*** chromosomes are again checked for dominance using Eq. 8 and new nondominated chromosomes are sorted out and given a front number, FRONT=2. Again, the new nondominated chromosomes (in FRONT 2) are given a dummy fitness value, F_2^*, which is slightly smaller than the lowest of the *shared* fitness values of the previous front. The sharing of the dummy fitness values is performed again, and a shared fitness value is assigned to each nondominated chromosome. This procedure is continued until all N_P chromosomes have been given a front number.

10. *Sharing* : Sharing is performed among the members of the i^{th} front (having n_i members) using the following procedure:

(a) For each chromosome, j, in front i, the dimensionless distance, d_{jk} , of this chromosome from any other chromosome, k , (including j) in the (same) front is calculated using

$$d_{jk} = \left\{ \sum_{l=1}^{N_{ga}} \left[\left(u_{P,l}^{(j)} - u_{P,l}^{(k)} \right) \Big/ \left(u_{P,l}^{max} - u_{P,l}^{min} \right) \right]^2 + \left[\left(T_J^{(j)} - T_J^{(k)} \right) \Big/ \left(T_J^{max} - T_J^{mm} \right) \right]^2 \right\}^{1/2} \qquad (9)$$

(b)We calculate the *niche count* , m_j , using

$$m_j = \sum_{k=1}^{n_i} Sh\left(d_{jk}\right) \qquad (10)$$

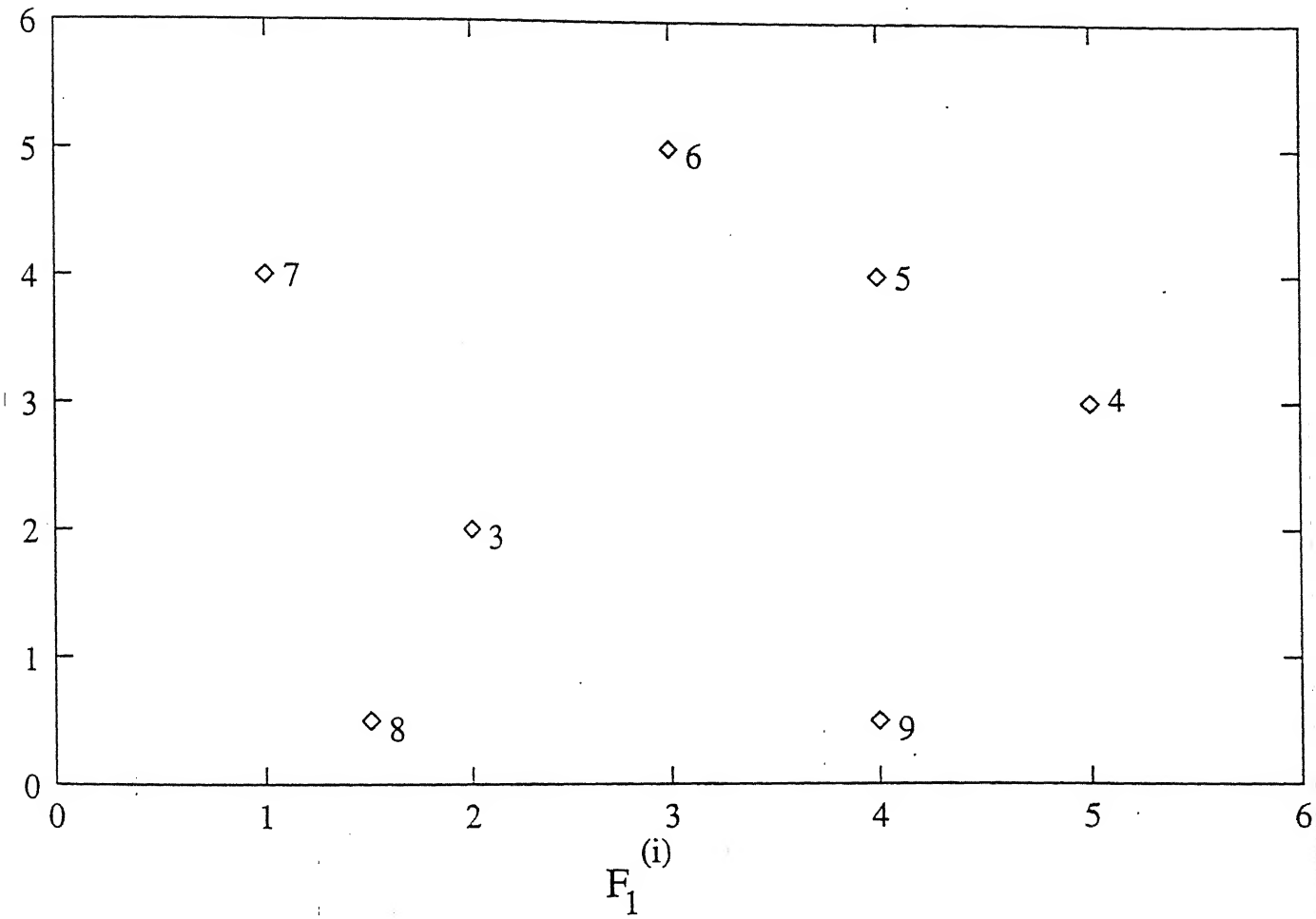

Fig. 3 : An example describing the concept of dominance .

where

$$Sh(d_{jk}) = \begin{cases} 1 - \left(\frac{d_{jk}}{\sigma_{share}}\right)^{\alpha}, & \text{if } d_{jk} < \sigma_{share}; \\ 0, & \text{otherwise.} \end{cases} \quad (11)$$

σ_{share} is given by

$$\sigma_{share} = \frac{1}{2q^{(1/(N_{ga}-1))}}. \quad (12)$$

In Eq. 12, q is the number of Pareto-optimal solutions desired (we have used q = 15 in our study). The parameter, α, is an exponent which controls the sharing effect (we have used $\alpha = 2$ in the present study).

(c) The dummy fitness, F_i^*, of each chromosome, j , in front, i , is modified by dividing F_i^* by the chromosome's niche count, m_j , to calculate the shared fitness value, $F_{ij}^{*'}$, as follows:

$$F_{ij}^{*'} = \frac{F_i^*}{m_j} \quad (13)$$

11. The stochastic remainder roulette wheel selection[20] is used on the shared fitness values, and a mating pool of N_P chromosomes is generated. This procedure involves proportionate selection, where first, the number of copies made of each chromosome is equal to the integer part of the value of $F_{ij}^{*'} / \overline{F}_{ij}^{*'}$. Here, $\overline{F}_{ij}^{*'}$ is the average of the shared fitness values of all the N_P chromosomes in the population. Additional copies of the $j^{th.}$ chromosome in the $i^{th.}$ front (to make a total of N_P in the mating pool) are made thereafter, using a roulette wheel with probability proportional to the fractional part of $F_{ij}^{*'} / \overline{F}_{ij}^{*'}$.

12. After the mating pool is created, crossover and mutation take place to produce the new population (next generation). These operations take place at the chromosome (binary)

level. Two chromosomes are randomly selected from the mating pool, a crossing site is selected (randomly again), and portions of the chromosomes before and after the crossing site are exchanged. For example, for seven-bit chromosomes with crossing site after the third binary, the crossover is described by the following :

$$\begin{array}{lll} 100 \mid 1111 & \longrightarrow & 100 \quad 0100 \\ 110 \mid 0100 & & 110 \quad 1111 \end{array} \qquad (14)$$

(old generation) (new generation)

While performning crossovers, only $p_c N_p$ chromosomes are crossed, the remaining being left untouched (p_c is referred to as the crossover probability).

Another operation, called mutation, is also used to improve the next generation. The mutation operator changes a binary number from 1 to 0 or vice versa, with a probability , p_m. This operation is carried out for each of the $N_p N_{chr}$ bits in the population, again using appropriate random numbers. The need for mutation leads to a local search around the current solution and helps maintain the diversity of the population.

This completes one generation of NSGA. These sets of operations are carried out from one generation to the next generation until the number of generations equals the maximum number of generations specified at the starting of the program as an input parameter.

In a nutshell, the feasible nondominated solutions are emphasized in every generation by the action of the reproduction operator of NSGA. Coexistence of multiple feasible nondominated solutions is ensured by using the sharing technique. Thereafter, crossover and mutation create new and, hopefully, better feasible nondominated solutions. This process continues and finally the best nondominated solutions of a population converge to the true Pareto-optimal solutions. Since diversity in the best feasible nondominated

solutions is maintained in each generation, the final population is expected to capture a number of different Pareto-optimal solutions simultaneously in one run.

Chapter 3

Results and Discussions

Several checks have been made to ensure that the computer code was free of errors. For example, the values of conv, $[C_2]$, μ_n , etc. , for any one chromosome were found to be the same as those obtained using our earlier[12] simulation code [with the same $V_T(t)$ and T_J]. Also, Pareto optimal solutions for some simpler problems[22] were obtained using our code, and they were found to be same as solutions obtained earlier. The CPU time ($[W]_0$ = 3.45%) for 20 generations was found to be 144 min. on a mainframe HP8000S/950 supermini computer.

The upper and lower limits of each of the N_{ga} control variables (for $[W]_0$ = 3.45%), $u_{P,k}^{max}$ and $u_{P,k}^{min}$, k = 1, 2,..., N_{ga} , as well as of the jacket fluid temperature, T_J^{max} and T_J^{min} , were first determined. It was found that these (slightly restricted) search 'windows' for $V_T/V_{T,max\_ref}$ and T_J were necessary, and that very large search domains on these two control variables led to severe computational problems with no Pareto solutions being obtained. Since our earlier multiobjective optimization study[28] of this reactor (with the *shape* of the pressure history fixed and described by four *values* only) gave us an optimal $V_T/V_{T,max\_ref}$ history and an optimal value of T_J , we selected the windows of these control variables around these previous solutions[28] as

$$0.4\times\left(V_T/V_{T,max,ref}\right)^{29} \le V_T/V_{T,max,ref} \le 1.6\times\left(V_T/V_{T,max,ref}\right)^{29} \qquad (15)$$

at corresponding values of t / t_f. The window for T_J was taken as $220^0 C \le T_J \le 270^0 C$. It was found that the window for $V_T/V_{T,max,ref}$ at $t / t_f = 0$ had to be widened beyond that given in Eq. 15, before solutions could be obtained. The exact window used for $V_T/V_{T,max,ref}$ is given in Table 3, while Fig. 4 gives the window as well as the optimal values obtained earlier.[28] Any further increase in the width of the window for $V_T/V_{T,max,ref}$ reduces the number of Pareto points obtained (without any change in the optimal solutions), and no further widening of the width of the window was attempted. The values of the computational parameters used in the optimization study are given in Table 4. The initial and other values associated with the reactor are the same as those given in Ref. 12.

Figs. 5 - 9 show the feasible solutions from generation to generation for $[W]_0 = 3.45\%$. Each of these points satisfy all the constraints of the system (Eqs. 6(d) - (f), and $\mu_n = \mu_{n,ref}$ within error bounds). Convergence to the optimal Pareto set is observed to take about 8 generations. The number of Pareto points obtained finally (ten) is found to be of the same order as q (15), as expected. The solution in Fig. 9 is referred to as the 'reference' run. The Pareto sets obtained for the other two water concentrations, i.e., $[W]_0 = 2.52\%$ and 4.43%, are given in Figs. 10 and 11. It may be added that the values of $[C_2]_{f,ref}$ are different for the three cases, while $t_{f,ref}$ is the same. The values of $u_{P,k}^{max}, u_{P,k}^{min}$ ($k = 1, 2, \ldots, N_{ga}$), T_J^{max} and T_J^{min}, as well as all the other computational parameters, for all these cases are taken to be the same as given in Table 3 and 4.

After the generations of the Pareto sets, a designer can choose an operating point (preferred solution) from these sets using his intuition (or other information not included in Eq. 6). One technique which can be used is to select the preferred solution as a point nearest to a point, U_i, called utopia. The points, U_i, are obtained by performing two

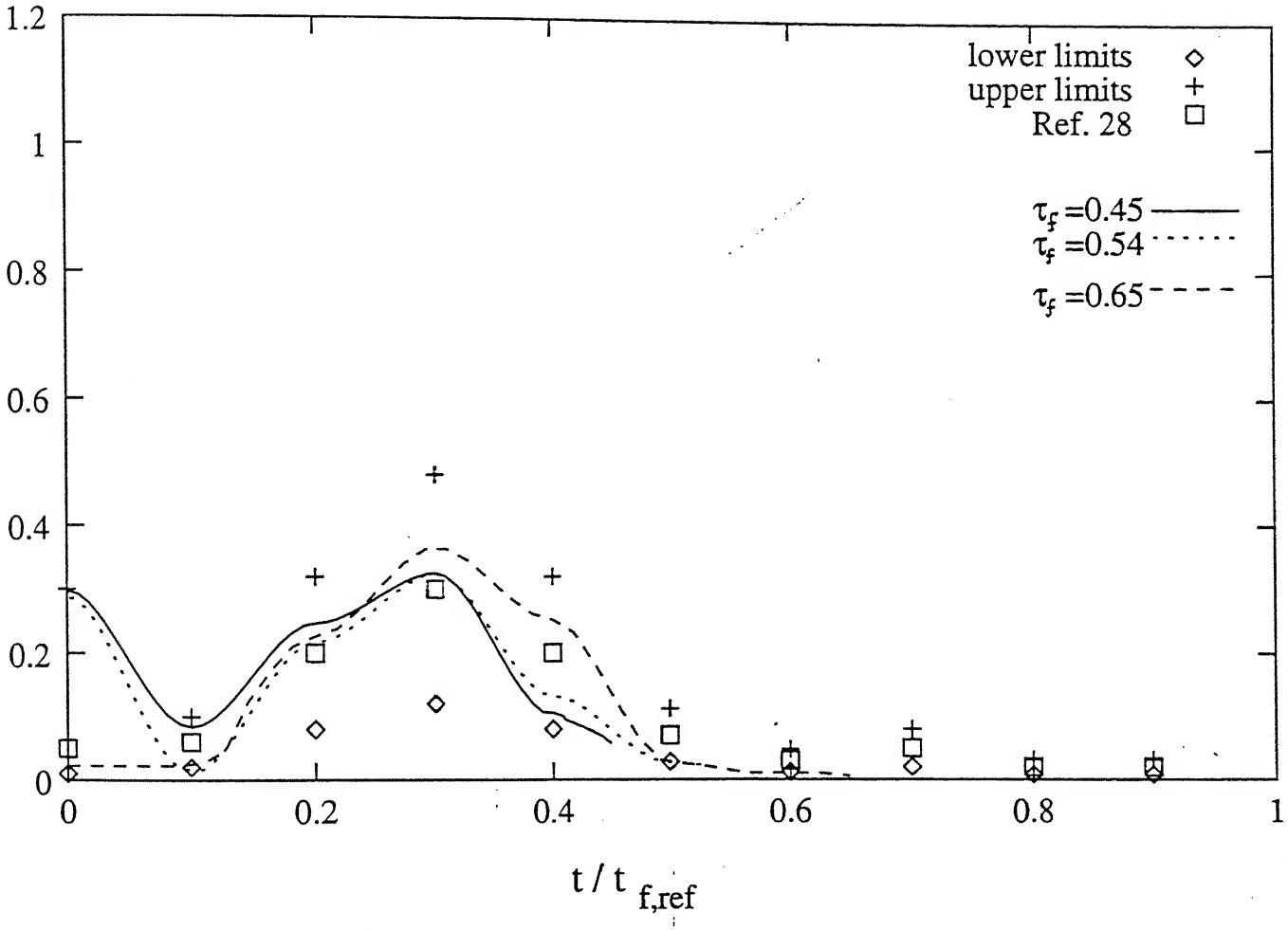

Fig. 4 : Dimensionless vapor release rate histories for $[W]_0$ = 3.45 %, for three points (t_f / $t_{f,ref}$ = 0.45, 0.54, 0.65) on the Pareto optimal set. and denote the lower and upper limits of the window used in this study, while denotes the optimal values of $V_T/V_{T,max,ref}$ as obtained in Ref. 28.

k^*	$(V_T^{max}/V_{T.max.ref})^{28}$	$(V_T^{max}/V_{T.max.ref})$	$(V_T^{min}/V_{T.max.ref})$
1	0.05	0.3	0.01
2	0.06	0.1	0.02
3	0.2	0.32	0.08
4	0.3	0.48	0.12
5	0.2	0.32	0.08
6	0.07	0.112	0.028
7	0.03	0.048	0.012
8	0.05	0.08	0.02
9	0.02	0.032	0.008
10	0.02	0.032	0.008

* $k = 1, 2, \ldots, N_{ga}$

Table 3: Window for $V_T / V_{T,max,ref}$ Used for our Study $[W]_0 = 3.45$ %.

$\left(V_T/V_{T,max,ref}\right)_k^{min,max}$, k = 1, 2, . . . , N_{ga} ; (as in Table 3)

$T_J^{max} = 270.0^0 C$

$T_J^{min} = 220.0^0 C$

$N_{ga} = 10$

$N_P = 80$

$N_{str} = 7$

$N_{sim} = 100$

$q = 15$

$\alpha = 2$

$p_c = 0.99$

$p_m = 0.001$

$N_{g,max} = 20$

$N_{chr} = (10+1) \times 7 = 77$

$w_1 = w_2 = 0.25 \times 10^6$

Table 4: Computational Parameters Used in the Reference Run

single objective function optimizations (i.e., by solving Eq. 6 using only one of the two objectives and dropping the other objective function completely). These two limiting solutions[28] show up as the straight lines in Figs. 9 - 11. The intersection of these lines gives the utopia. Point U_i is unattainable, but represents an ideal. The preferred solution is often taken[2,3] to be the point nearest to utopia. These points are denoted by O_i in Figs. 9 - 11. The subscript, i , on points U_i and O_i corresponds to the integer in the value of the initial water concentration, $[W]_0$. It must be emphasized that the geometrical construction required to obtain points O_i will depend on the scales being used in plotting the Paretos. However, this is the best one can do in absence of additional information.

Each point on the Pareto sets in Figs. 9 - 11 corresponds to a different $V_T/V_{T,max,ref}$ history as well as T_J. Three of these histories (for $t_f / t_{f,ref} = 0.45, 0.54, 0.65$ on the Pareto for the reference case of $[W]_0 = 3.45\%$) are shown in Fig. 4. Fig. 12 shows the optimal values of T_J corresponding to the Paretos for all three values of $[W]_0$.

In Fig. 13, the computed Pareto sets are compared with the Pareto sets obtained by Sareen and Gupta[28] for one case. The Paretos obtained in the present case indicate superior performance compared to that obtained earlier. This indicates that 'freezing' of the *shape* of the pressure history during optimization does not give the best optimal solutions, since the search space gets limited by this procedure, a drawback that does not exist in the current, more general, study.

Fig. 14, shows the optimal history of $V_T/V_{T,max,ref}$ for the preferred solution, O_3, and compares it with values currently in use.[12] It is observed that the vapor release rate is finite at the beginning in the case of the optimal solution, in contrast to the present operation. Also, the maximum value of the optimal vapor release rate is lower. Fig. 15 shows that higher vapor release rates are required for higher values of $[W]_0$. Fig. 2 shows the variation of the dimensionless pressure, Π, with dimensionless time for the preferred

solutions (O_2 - O_4). Much lower pressures are required as compared to the current operation. Fig. 16 shows the variation of the dimensionless temperature with dimensionless time for the three preferred solutions. The rise of the temperatures are observed to increase more slowly as compared to current values. This is because of nonzero vapor release rates at the beginning (leading to higher amounts of vaporization). In Fig. 17, the number average chain length, μ_n , *vs.* the dimensionless time, is plotted for the three preferred solutions. The plateau observed currently is found to be missing in the case of the optimal runs. This is similar to the observation made by Sareen and Gupta.[28] In Fig. 18, the monomer conversion, conv, is plotted against the dimensionless time. Delayed attainment of the equilibrium values is observed. In Fig. 19, $[C_2]/[C_2]_{f,ref,3}$ (where subscript 3 indicates that the reference value, $[C_2]_{f,ref}$, for $[W]_0 = 3.45\%$ is used for all three values of $[W]_0$) is plotted against the dimensionless time for the preferred solutions as well as for the current operation. Use of the same denominator for all three $[W]_0$ helps compare the values of $[C_2]$ better. It is observed that the amount of cyclics are much smaller than produced currently, as also indicated in Fig. 13. The quality of the product produced under optimal conditions is, thus, observed to be far better (while the total reaction time, t_f, is also substantially reduced leading to higher plant capacities).

The effect of varying the several computational parameters given in Table 3 and 4 on the Pareto solution for $[W]_0 = 3.45\%$ was then studied. If the population size, N_P , is decreased from the reference value of 80 to 60, the same Pareto is obtained. We could, as well, choose to use $N_P = 60$ since the number of function evaluation would be lower. However, increase in N_P to 100 led to severe memory and CPU time requirements, and only three generations could be studied. A few extra feasible solutions were found for $N_P = 100$ than shown in Figs. 5 - 8. The evolving Pareto appeared to be identical. On increasing the value of N_{str} from 7 to 10, we obtained Pareto solutions which differed only in the fifth

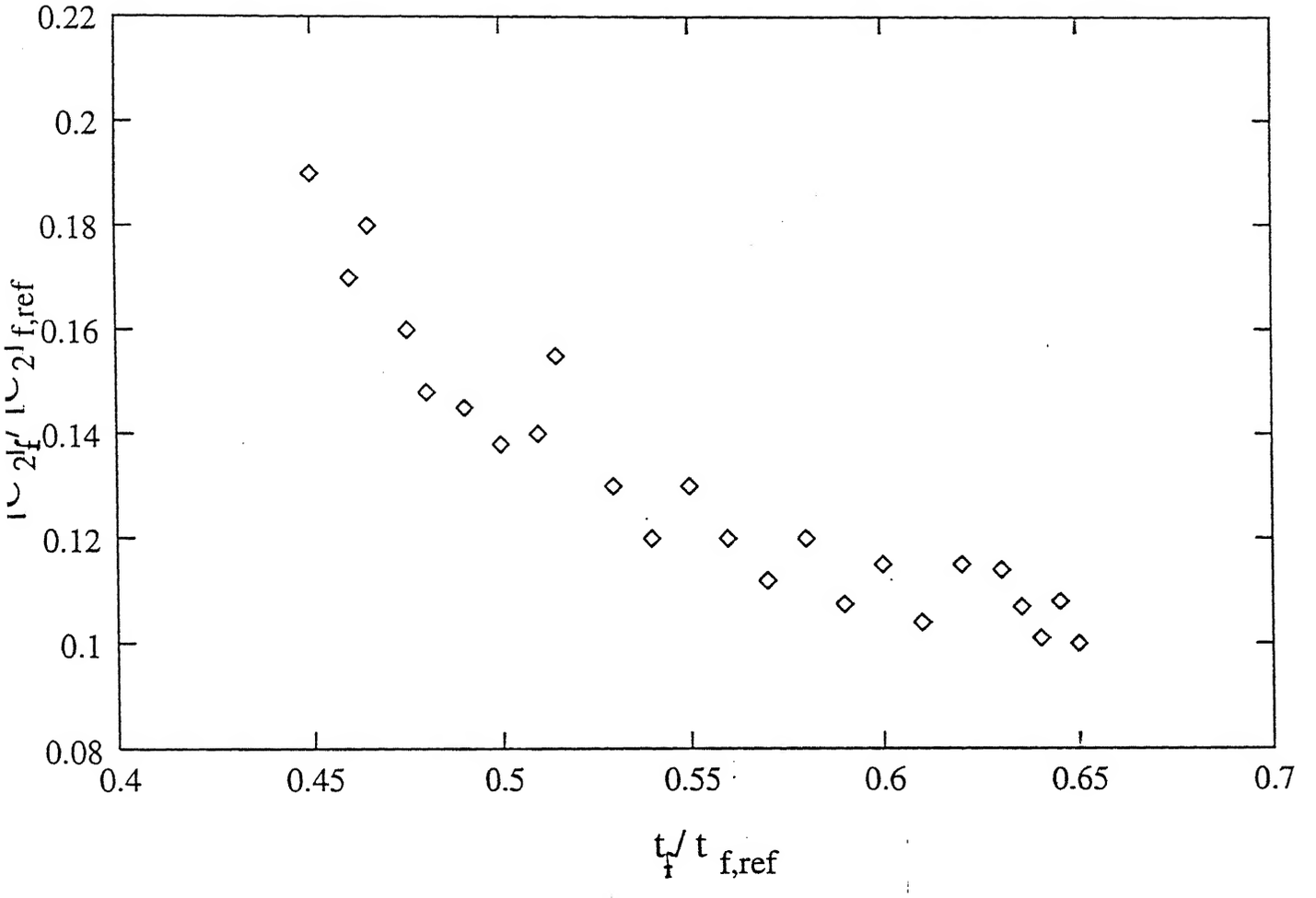

Fig. 5 : Feasible points at generation number = $N_g = 0$, for $[W]_0 = 3.45$ % .

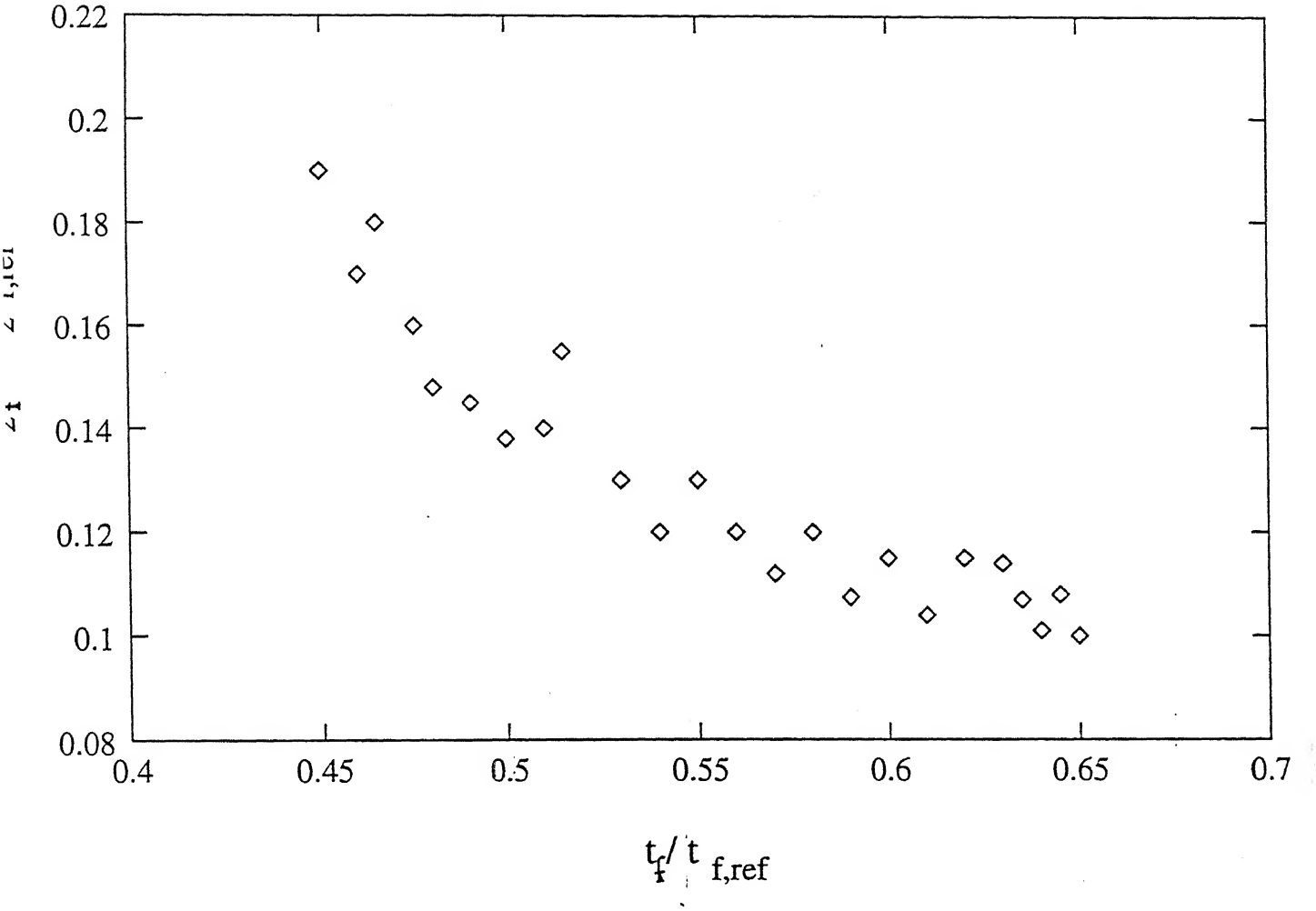

Fig. 6 : Feasible points at generation number = $N_g = 1$, for $[W]_0 = 3.45$ % .

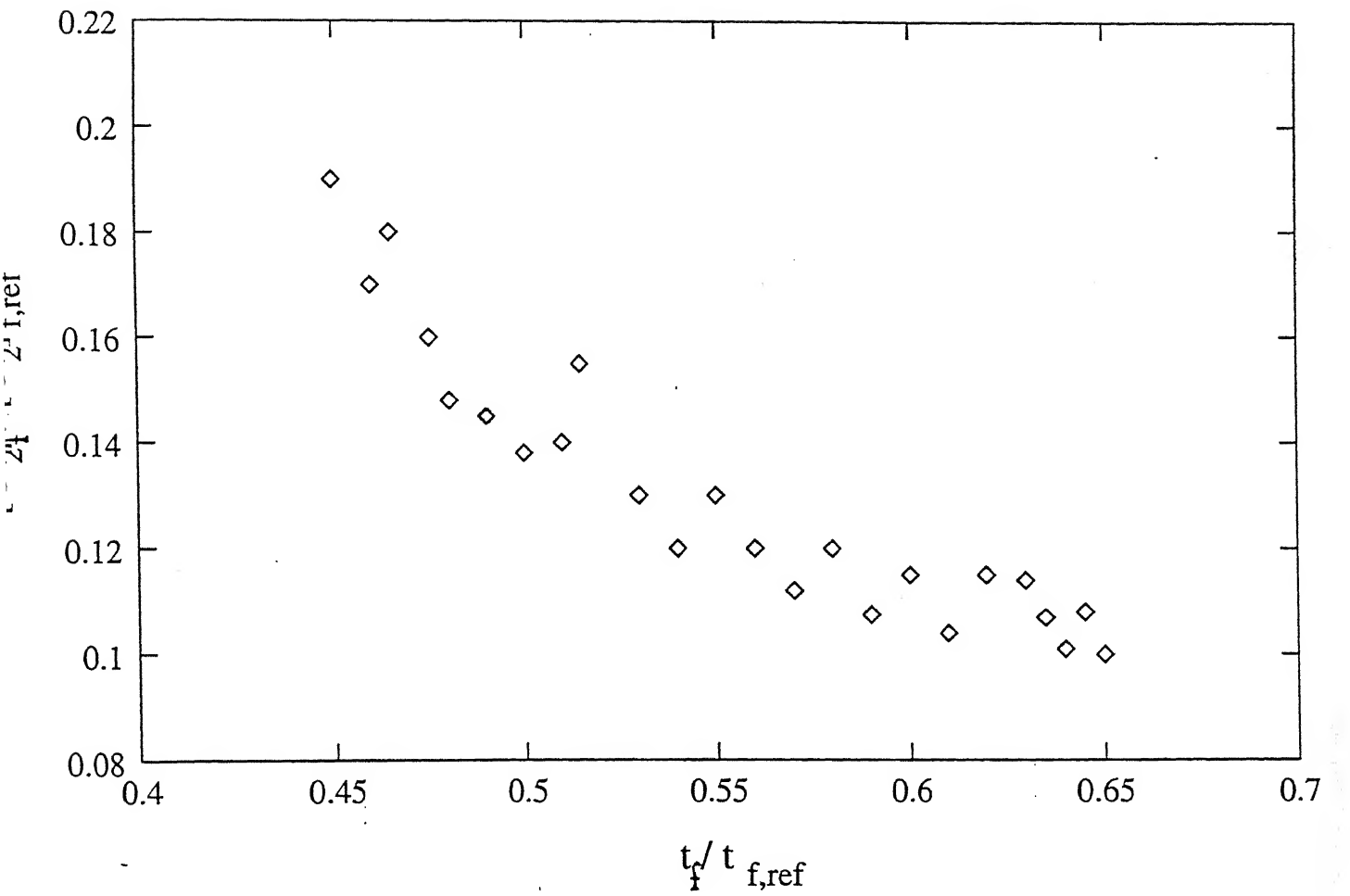

Fig. 7 : Feasible points at generation number = $N_g = 2$, for $[W]_0 = 3.45$ % .

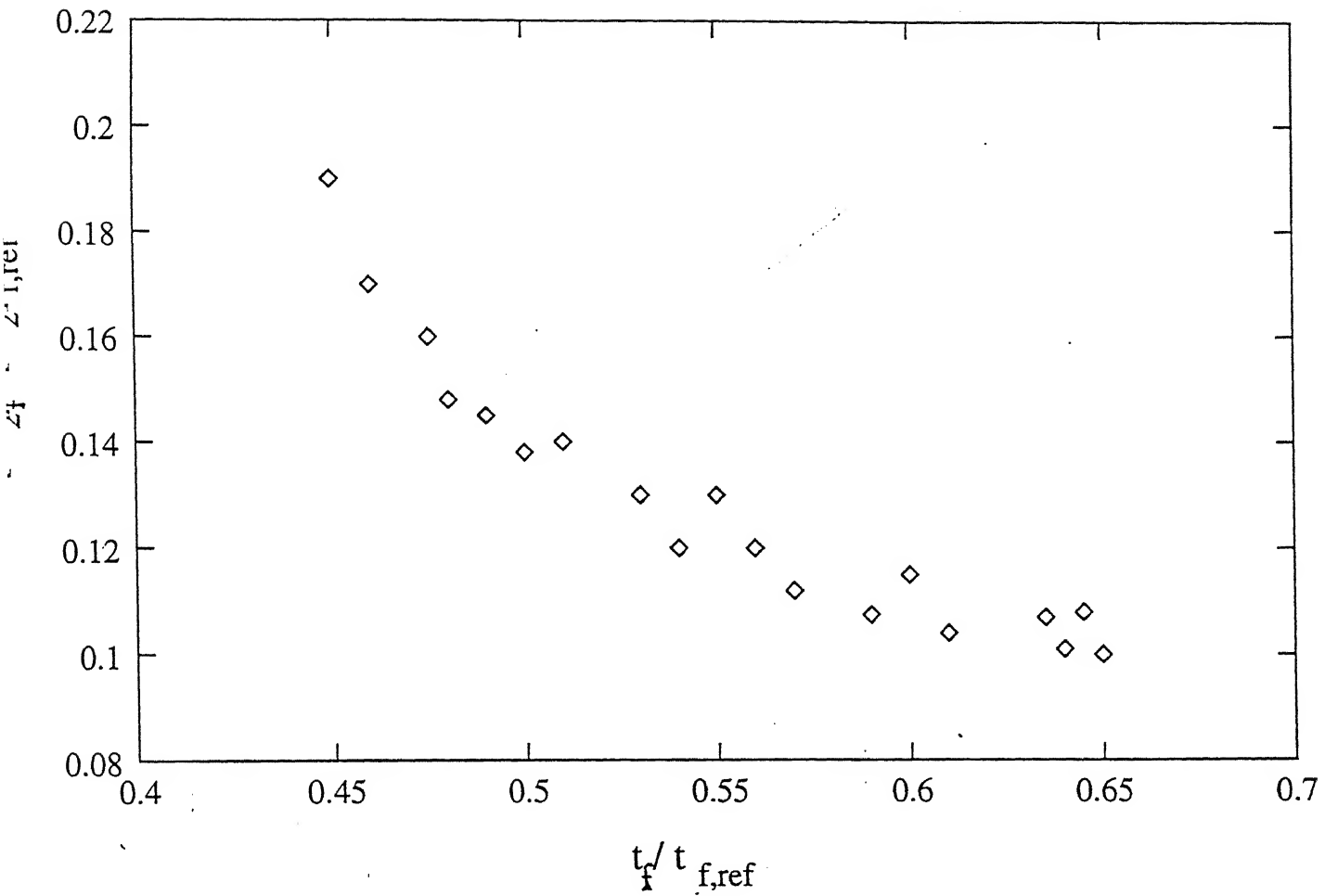

Fig. 8 : Feasible points at generation number = $N_g = 5$, for $[W]_0 = 3.45$ % .

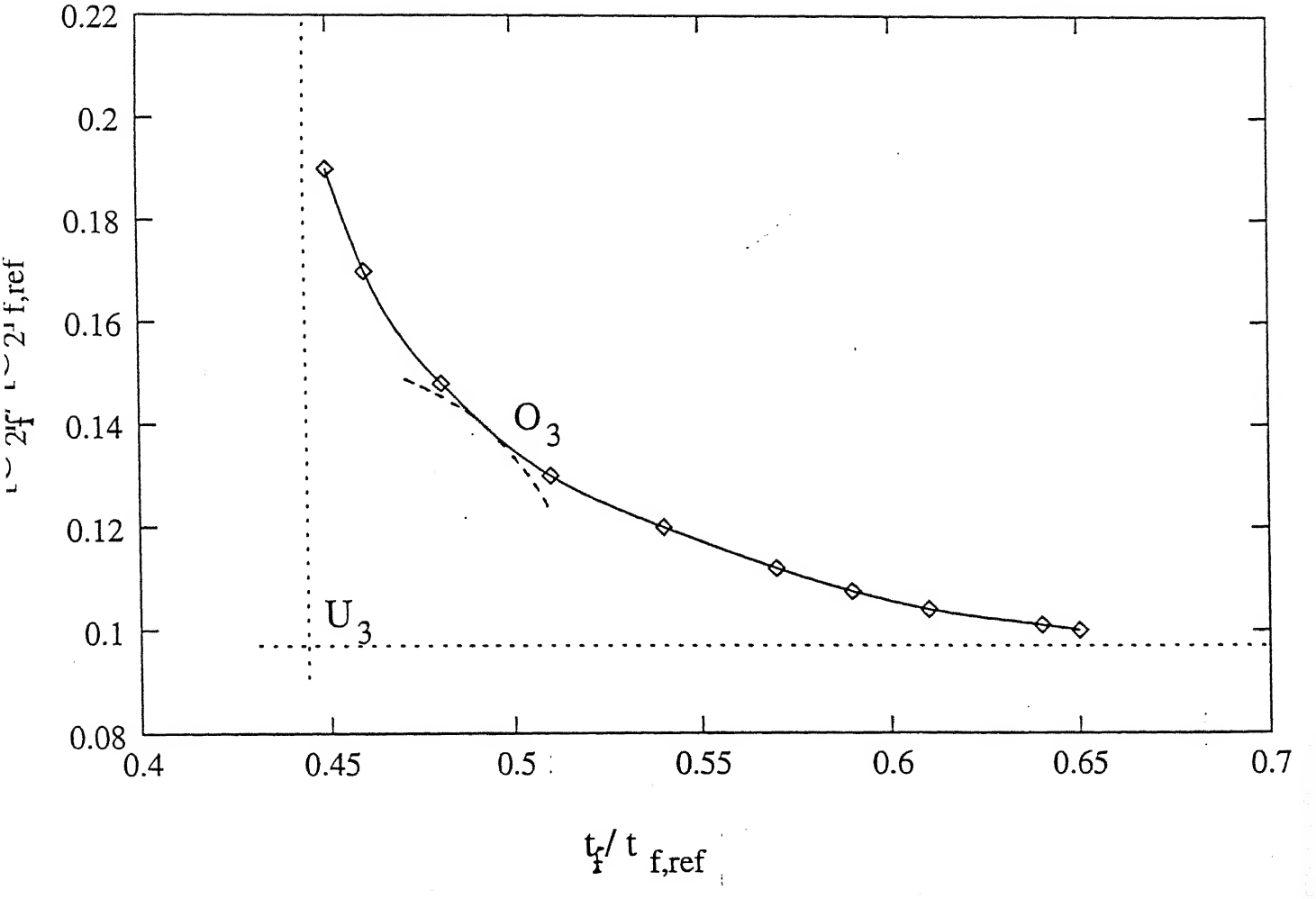

Fig. 9 : Pareto optimal set (for N_g = 8 as well as 20) for $[W]_0$ = 3.45 %. U_3 is the utopia while O_3 is the preferred solution .

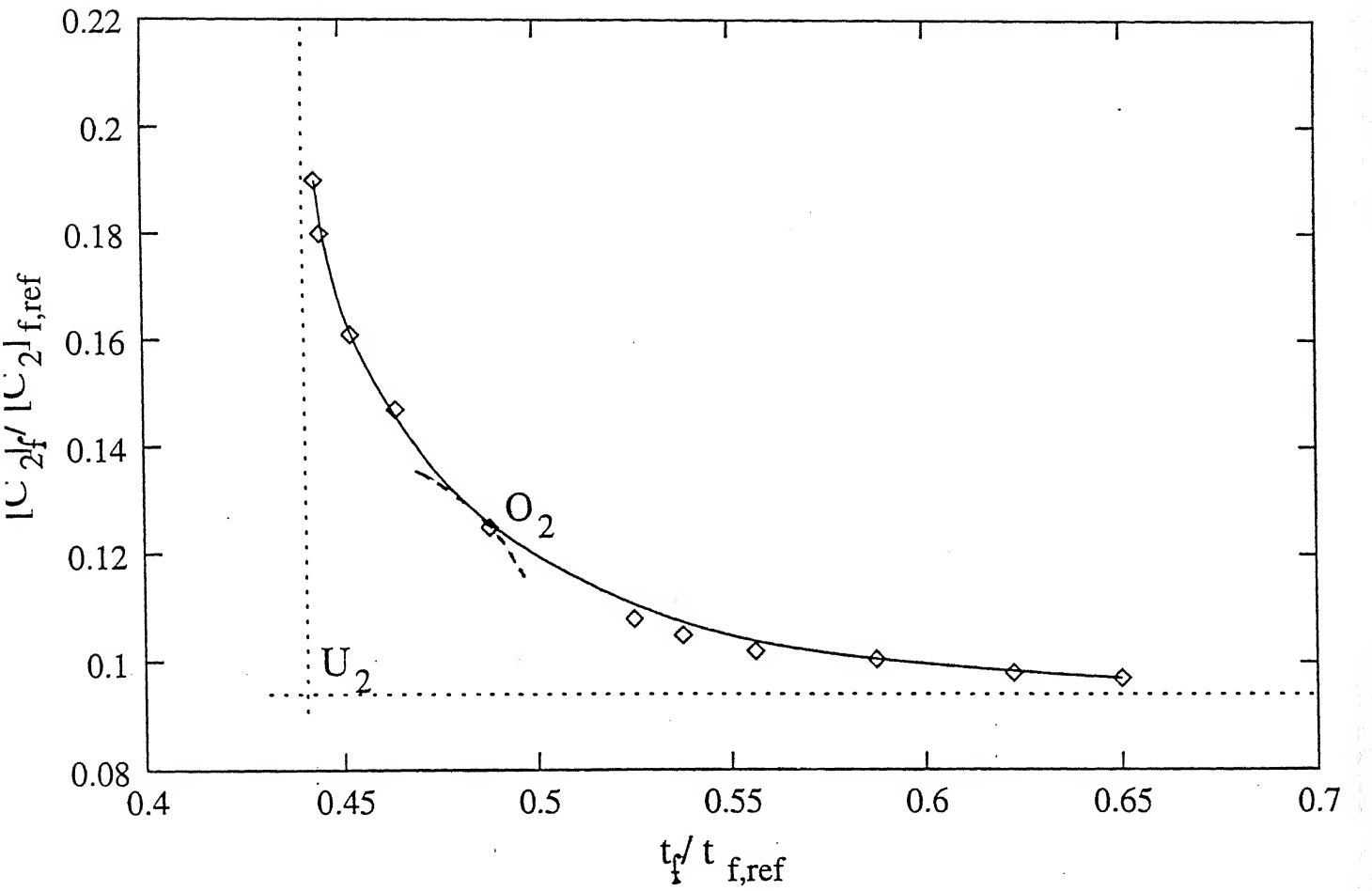

Fig. 10 : Pareto optimal set (for $N_g = 7$ as well as 20) for $[W]_0 = 2.52$ %. U_2 is the utopia while O_2 is the preferred solution .

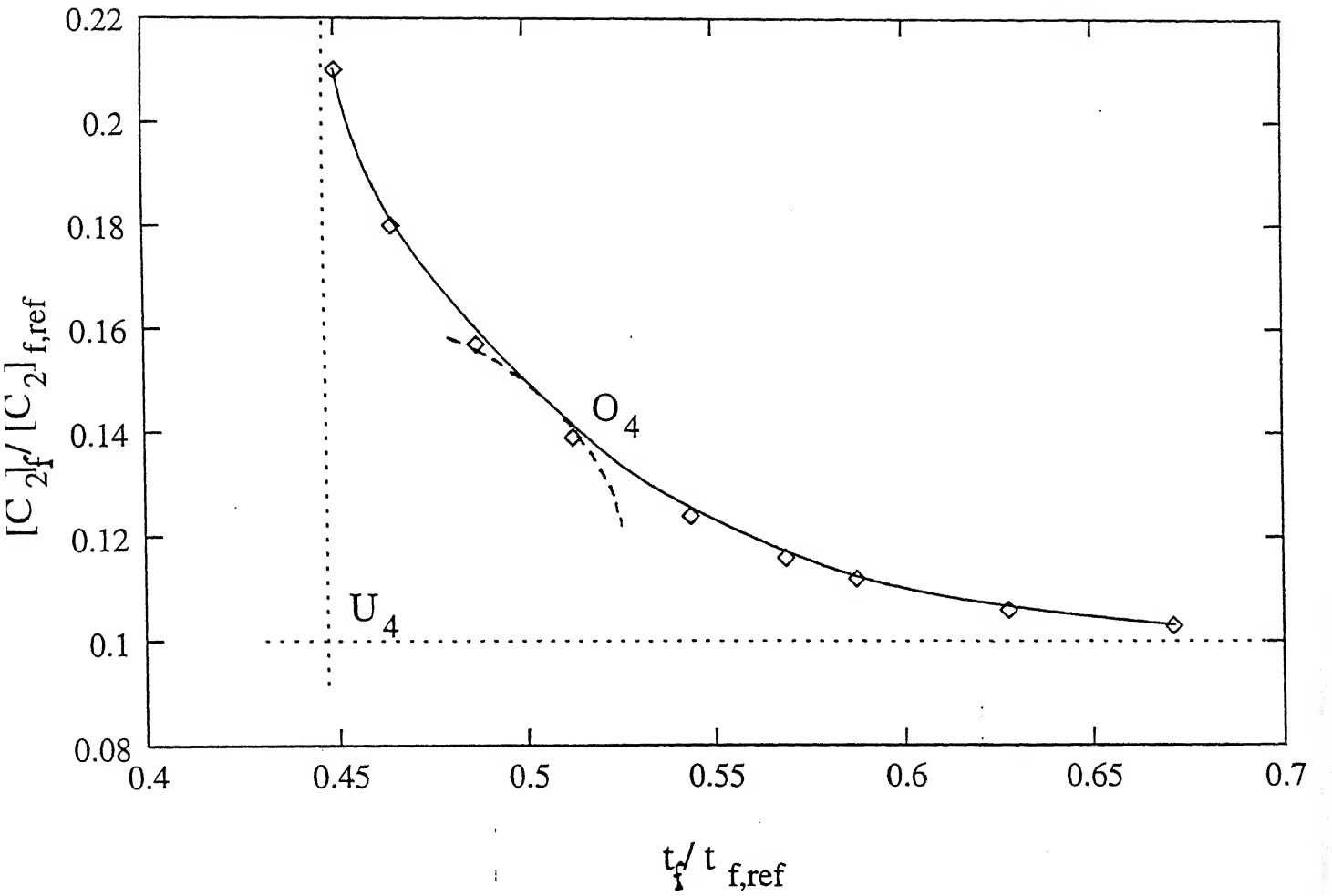

Fig. 11 : Pareto optimal set (for $N_g = 10$ as well as 20) for $[W]_0 = 4.43$ %. U_4 is the utopia while O_4 is the preferred solution .

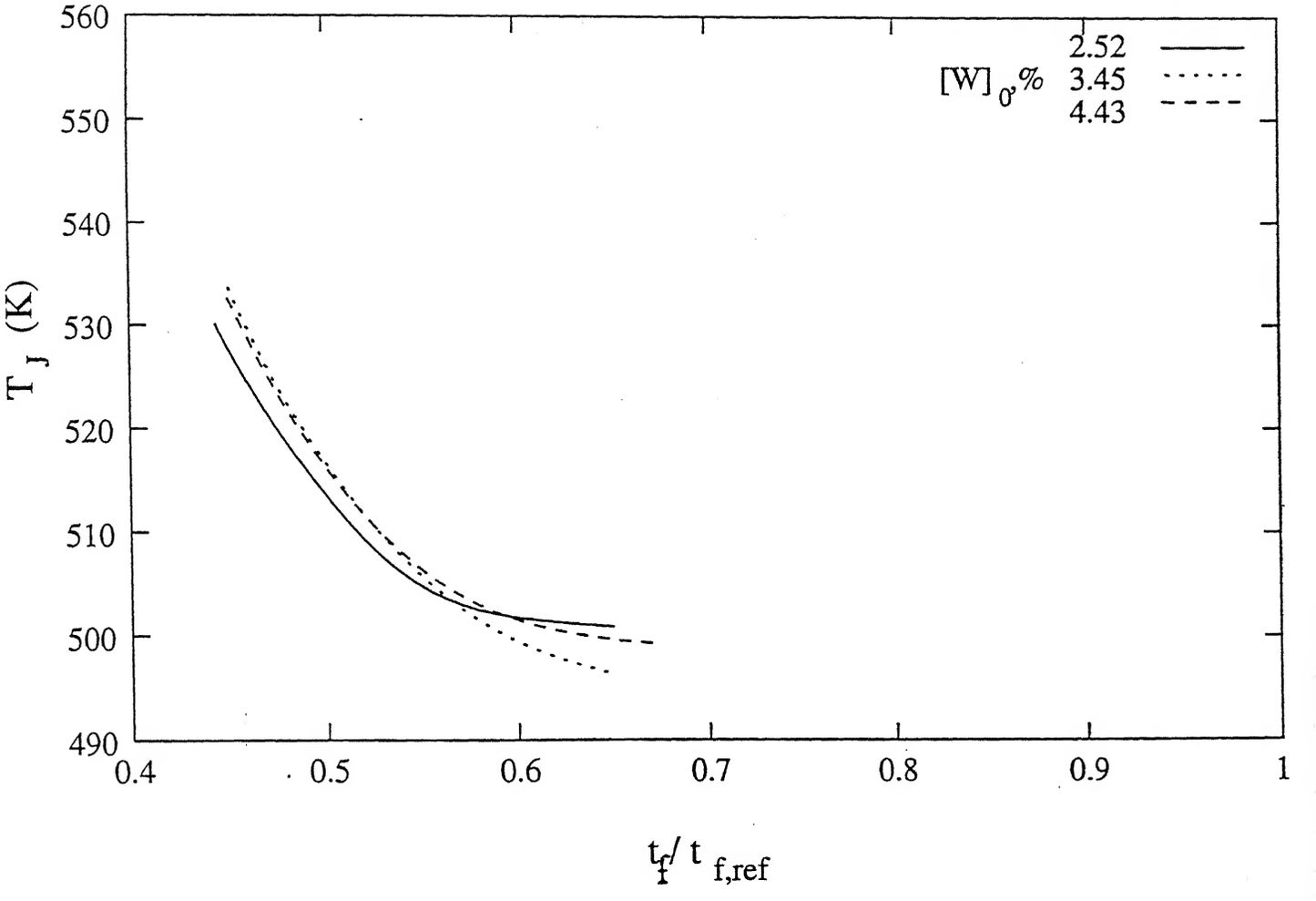

Fig. 12 : Jacket fluid temperatures corresponding to different points on the three Paretos .

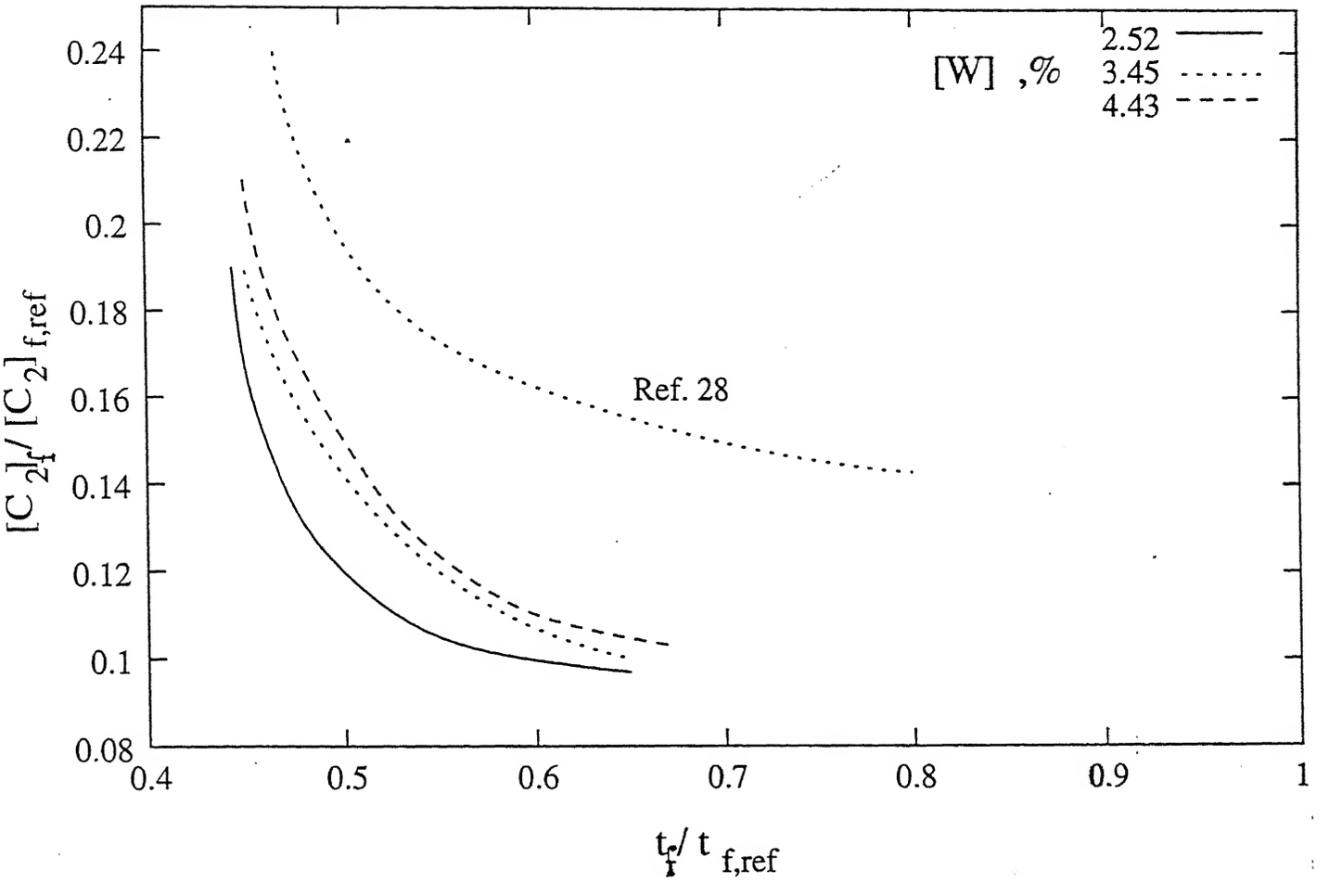

Fig. 13 : Comparison of the three Paretos with the Pareto for $[W]_0$ = 3.45 % obtained by Sareen and Gupta.[28]

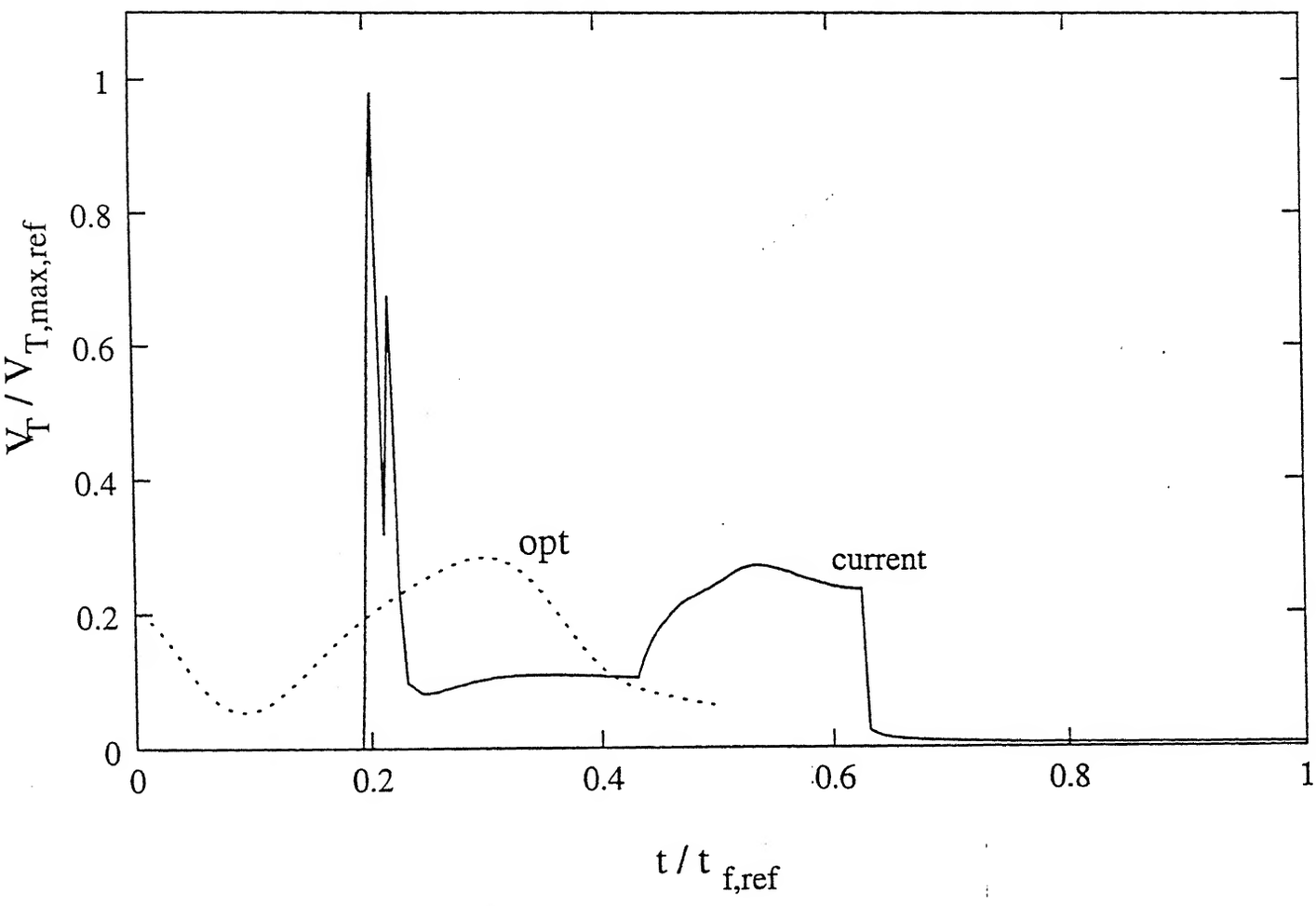

Fig. 14 : Variation of the dimensionless vapor release rate with dimensionless time for the current and optimal (preferred solution, O_3) cases; $[W]_0 = 3.45\%$.

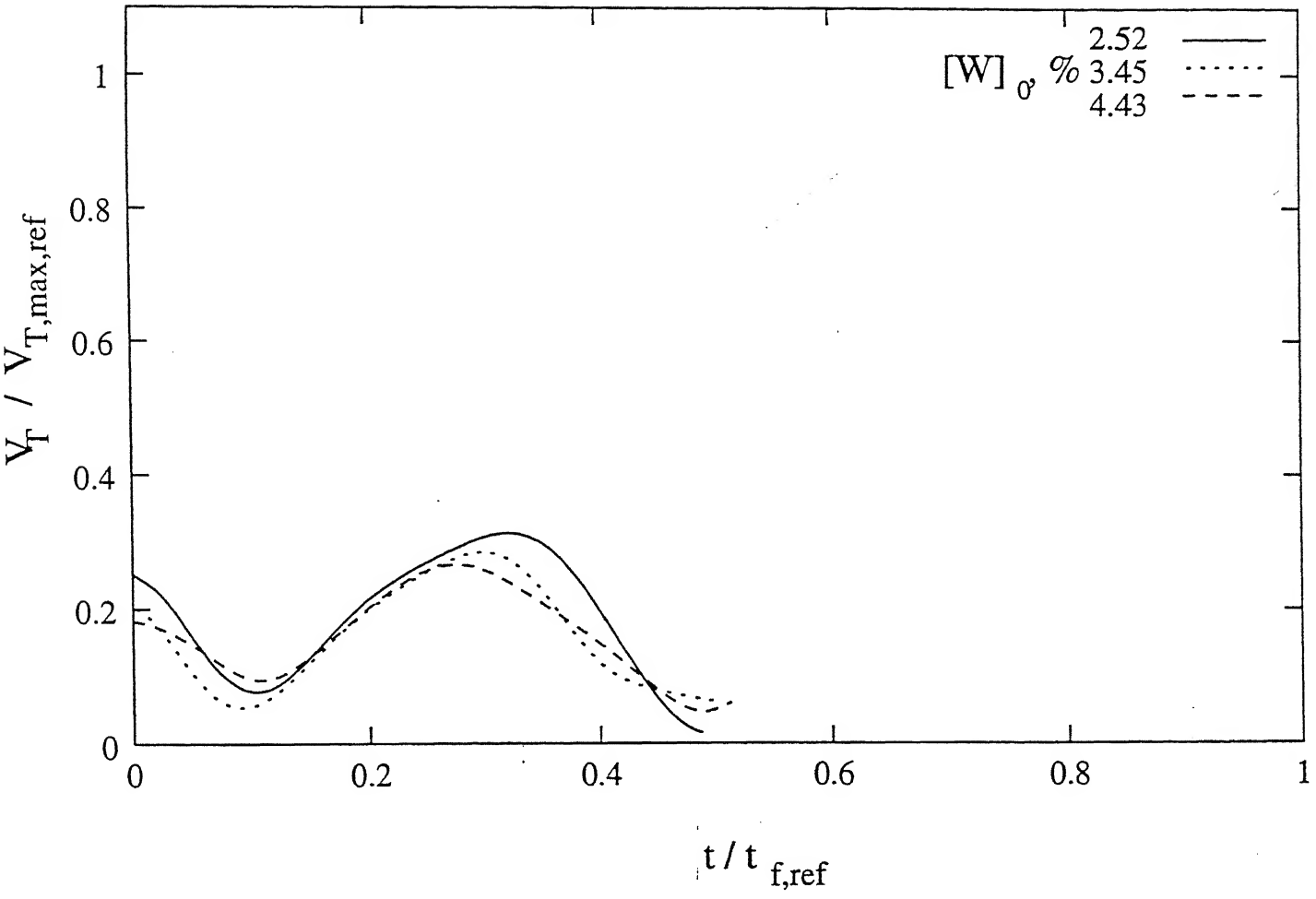

Fig. 15 : Dimensionless vapor release rate histories for the preferred solutions for $[W]_0$ = 2.52%, 3.45%, 4.43% .

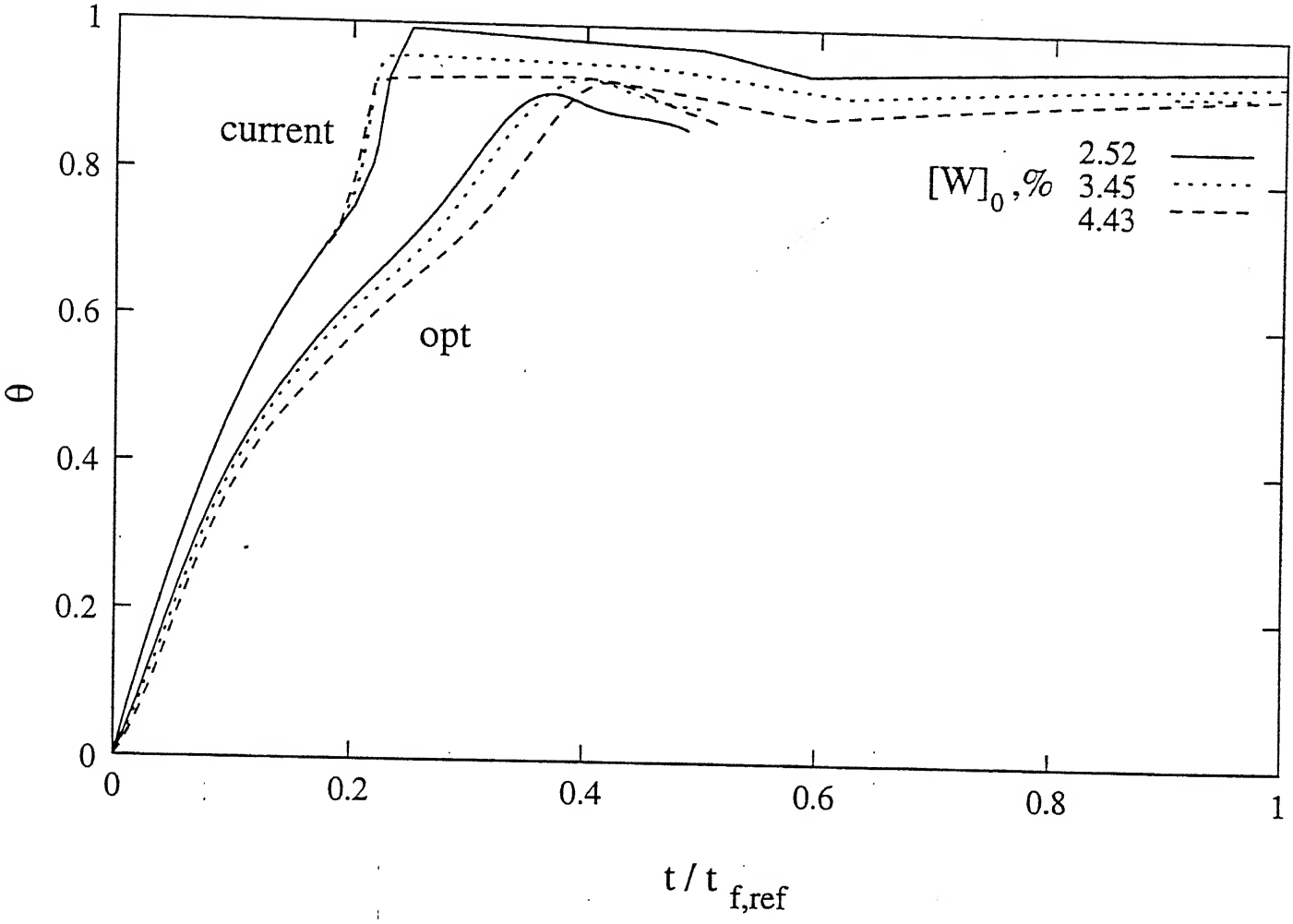

Fig. 16 : Variation of the dimensionless temperature with dimensionless time for the current and optimal (preferred solutions) cases, for $[W]_0$ = 2.52%, 3.45%, 4.43% .

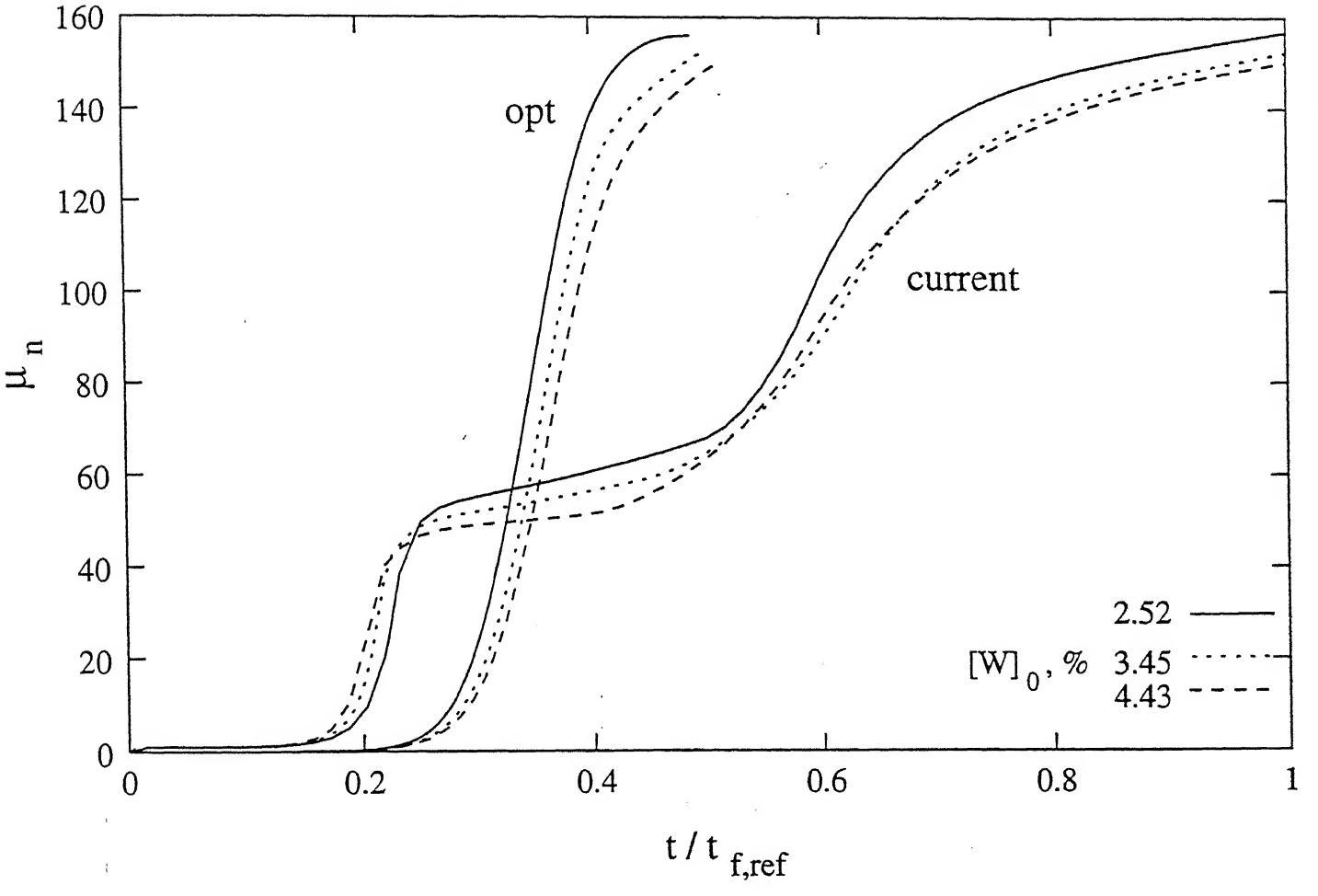

Fig. 17 : Variation of the degree of polymerization with dimensionless time for the current and optimal (preferred solutions) cases, for $[W]_0 = 2.52\%, 3.45\%, 4.43\%$.

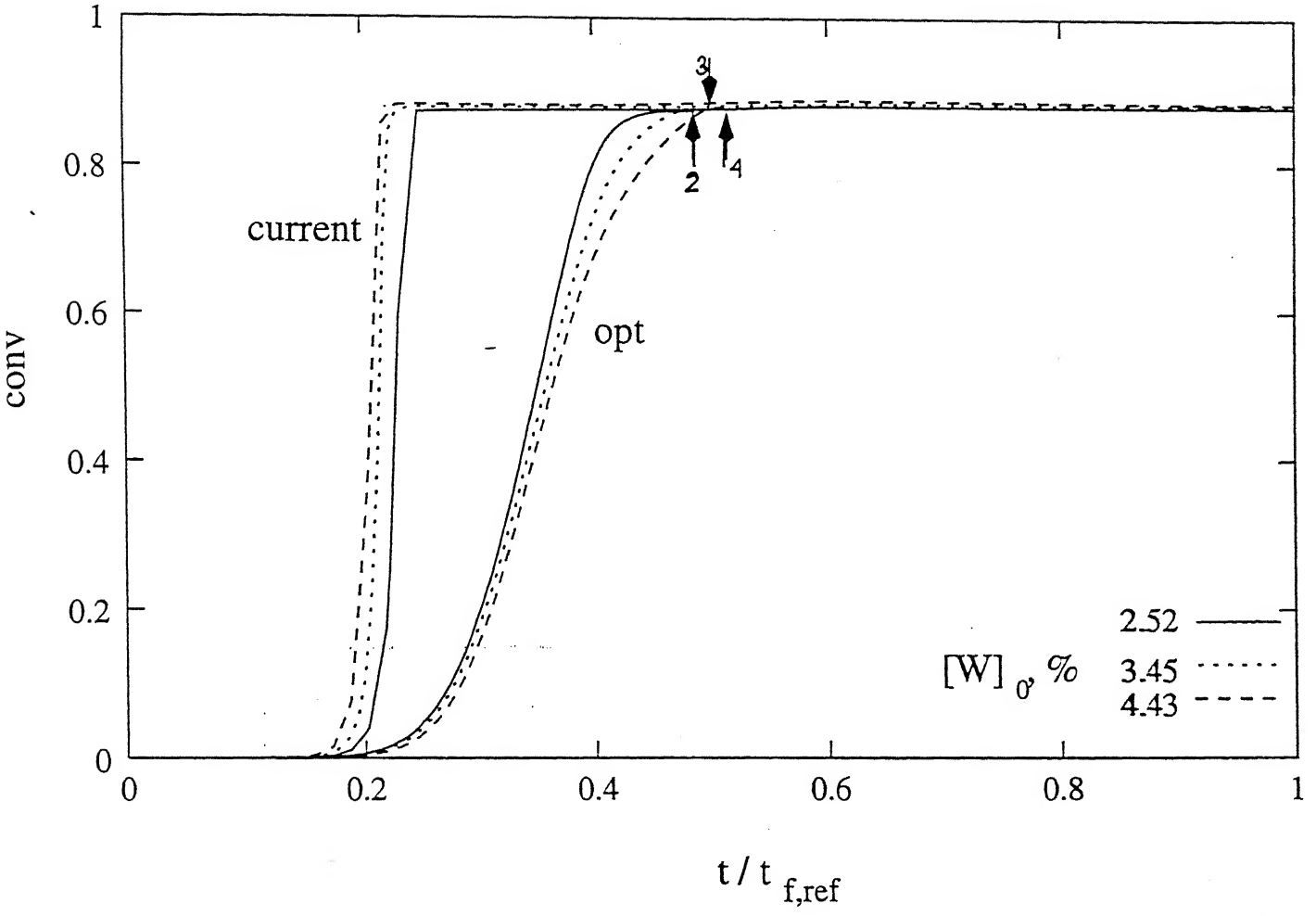

Fig. 18 : Variation of the monomer conversion with dimensionless time for the current and optimal cases (preferred solutions), for $[W]_0 = 2.52\%, 3.45\%, 4.43\%$.

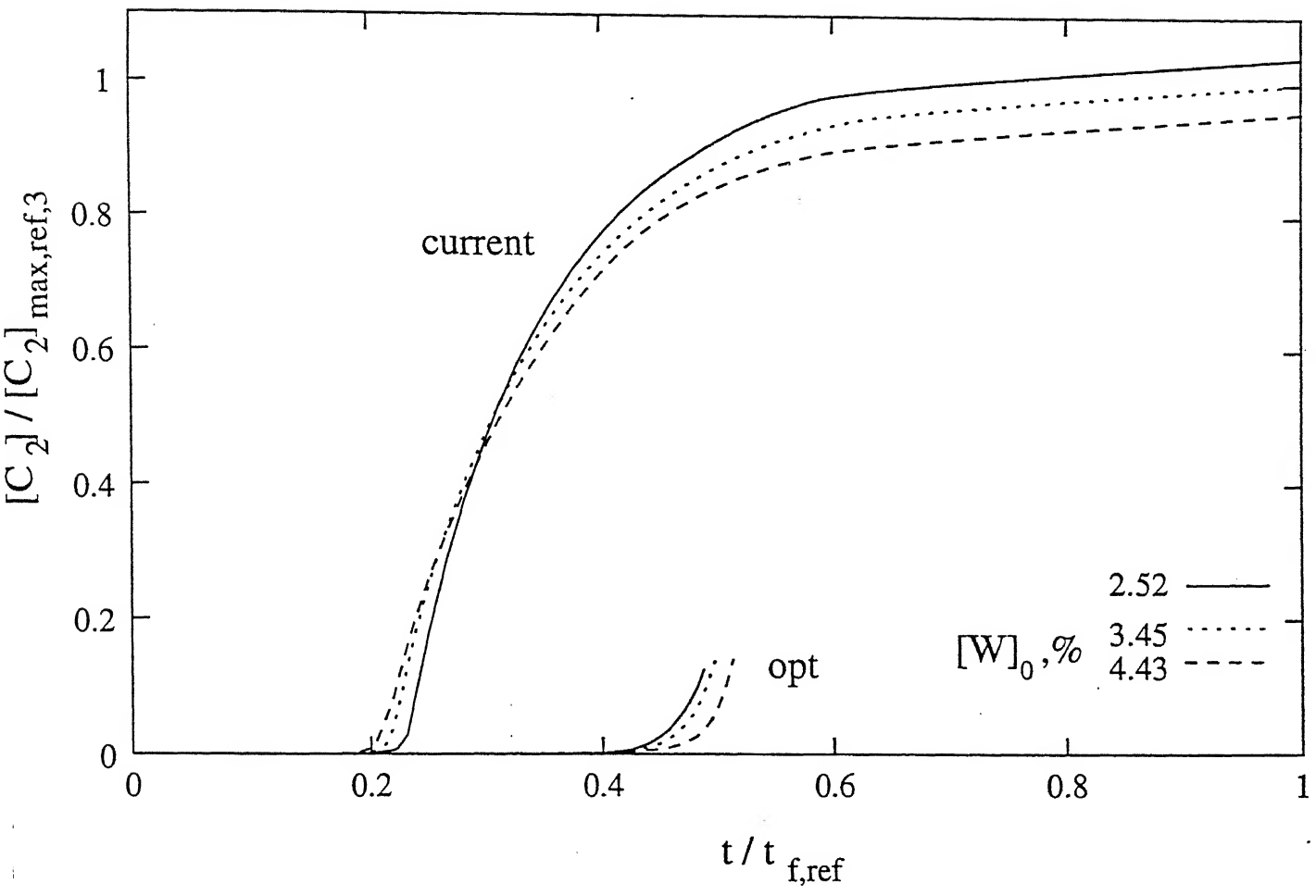

Fig. 19 : Variation of the dimensionless dimer concentration (using $[C_2]_{f,ref}$ for $[W]_0$ = 3.45% as the normalizing parameter for all three cases) with dimensionless time for the current and optimal cases (preferred solutions), for $[W]_0$ = 2.52%, 3.45%, 4.43% .

to seventh decimal places. This increased accuracy is, thus, not necessary and the reference value $N_{str} = 7$ is alright. Similarly, increase in the value of N_{ga} from 10 to 16 led to no significant changes in the Pareto set. The effect of varying the value of the crossover probability, p_c, from 0.99 to 0.77, again, led to no significant changes in the optimal solutions. The effect of a change in the value of the mutation probability, p_m, from 0.001 to 0.1, led to fewer points on the Pareto set (but the ones obtained were identical to those in the reference case), but convergence was attained more slowly (at the 18th. generation). Also, higher p_m led to some erratic behavior in the feasible points obtained in each generation in the beginning (this was probably the cause of slow convergence). Decrease as well as minor increase of the window provided for $V_T/V_{T,max,ref}$ (to factors of 0.2 and 1.2 or 0.7 and 1.7, of the values in Ref. 28) led to fewer points on the Pareto (through the same values were obtained for the points). The reference values of the computational parameters in Tables 3 and 4, thus, appear justified.

Chapter 4

Conclusions

Pareto optimal solutions have been obtained for the multiobjective optimization problem described in Eq. 6. The vapor release rate *history*, $V_T(t)$, and the value of the jacket fluid temperature ,T_J, have been used as the control (optimizing) variables. An adapted NSGA (Nondominated Sorting Genetic Algorithm) technique has been used to obtain the solutions. Use of this niche based search technique was found to be superior to the use of Pontryagin's minimum principle for dynamic optimization.[29] In fact, our attempt to extend our earlier work[29] using Pontryagin's principle (for single objective optimization of the semibatch nylon 6 reactor) to the more difficult problem described in Eq. 6, failed due to severe numerical problems. This indicates the superiority of the present technique. It is found that there is considerable scope for improvement in the operation of the industrial reactor (reduced total reaction times, reduced cyclic formation, while simultaneously maintaining the values of monomer conversion and the number average molecular weight). We understand that some improvements have already taken place on the industrial reactor recently, along the lines indicated in the present work. This work has been partly funded by a grant from the Research Centre, Gujrat State Fertilizers Co. Ltd., Vadodara, India.

Chapter 5

Suggestions For Future Work

Though this work has predicted considerable improvement in the performance of the industrial semibatch nylon 6 reactor, a more fundamental optimization study is called for. Industrial implementation of optimum vapor release rate histories or pressure histories, predicted by our work may not be an easy task, if the industrial reactor studied here is not capable of taking care of very sophisticated control.

It is well known that good models are a prerequisite for any optimization study. In this study, the activity coefficients of the monomer and water used were those obtained[12] by curve-fitting plant-data under one set of operating conditions. It is necessary to re-confirm whether the coefficients used in the expressions of γ_m and γ_w are applicable under the different conditions corresponding to the optimal solutions. Use of more fundamental relationships for the activity coefficients could also to be studied.

References

[1] J. N. Farber, in *Handbook of Polymer Science and Technology*, N. P. Cheremisinoff, Ed., Marcel Dekker, New York, 1989, Vol. 1, p. 429.

[2] Y. Y. Haimes, *Heirarchial Analysis of Water Resources Systems*, McGraw-Hill, New York, 1977.

[3] V. Chankong and Y. Y. Haimes, *Multiobjective Decision Making-Theory and Methodology*, Elsevier, New York, 1983.

[4] R.M.Wajge and S.K.Gupta, *Polym. Eng. Sci.*, **34**, 1161 (1994).

[5] A. Tsoukas, M. Tirrel, and G. Stephanopoulos, *Chem. Eng. Sci.*, **37**, 1785 (1982).

[6] L. T. Fan, C. S. Landis, and S. A. Patel, in *Frontiers in Chemical Reaction Engineering*, L. K. Doraiswamy and R. A. Mashelkar, Eds., Wiley Eastern, New Delhi, 1984, p. 609.

[7] J. N. Farber, *Polym. Eng. Sci.*, **34**, 1161 (1994).

[8] D. Butala, K. Y. Choi, and M. K. H. Fan, *Comput. Chem. Eng.*, **12**, 1115 (1988).

[9] S. S. S. Chakravarthy, D. N. Saraf and S. K. Gupta, *J. Appl. Polym. Sci.*, **63**, 529 (1997).

[10] A. Gupta, S. K. Gupta, K. S. Gandhi, M. H. Mehta, M. R. Padh, A. V. Soni and B. V. Ankleswaria, *Chem. Eng. Commun.*, **113**, 63 (1992).

[11] A. Gupta, S. K. Gupta, K. S. Gandhi, M. H. Mehta, M. R. Padh, A. V. Soni and B. V. Ankleswaria, in *Recent Trend in Chemical Reaction Engineering*, B. D. Kulkarni, R. A. Mashelkar, and M. M. Sharma, Eds., Wiley Eastern, New Delhi, 1987, p. 281.

[12] R.M.Wajge, S.S.Rao and S.K.Gupta, *Polymer*, **35**, 3722 (1994).

[13] W.H.Ray and J.Szekely, *Process Optimization*, Wiley, New York, 1969.

[14] L. Lapidus and R. Luss, *Optimal Control of Engineering Processes*, Blaisdell, Waltham, MA, 1967.

[15] N. R. Vaid and S. K. Gupta, *Polym. Eng. Sci.*, **31**, 1708 (1991)

[16] A.K.Ray and S.K.Gupta, *J Appl. Polym. Sci.*, **30**, 4529 (1985).

[17] A.K.Ray and S.K.Gupta, *Polym. Eng. Sci.*, **26**, 1033 (1986).

[18] D.Srivastava and S.K.Gupta, *Polym. Eng. Sci*, **31**, 596 (1991).

[19] J.H.Holland, *Adaptation in Natural and Artificial Systems*, Univ. Michigan Press, Ann Arbor, MI, 1975.

[20] D.E.Goldberg, *Genetic Algorithms in Search, Optimization and Machine Learning*, Addison-Wesley, Reading, MA, 1989.

[21] K. Deb, *Optimization for Engineering Design: Algorithms and Examples*, Prentice Hall of India, New Delhi, 1995.

[22] N. Srinivas and K. Deb, *Evolutionary Computation*, **2**, 3 (1995).

[23] H. K. Reimschuessel, J. Polym. Sci., *Macromol. Rev.*, **12**, 65 (1977).

[24] K. Tai and T. Tagawa, *Ind. Eng. Chem. Prod. Res. Dev.*, **22**, 192 (1983).

[25] A. Kumar and S. K. Gupta, *J. Macromol. Sci., Revs. Macromol. Chem. Phys*, **C 26**, 183 (1986).

[26] S.K.Gupta, *Numerical Methods for Engineers*, New Age International/Wiley Eastern,New Delhi, 1995.

[27] K. Deb, *Genetic Algorithms in Multimodal Function Optimization* . MS thesis, University of Alabama (TCGA Report No. 89002). The Clearinghouse for Genetic Algorithms,University of Alabama,Tuscaloosa (1989).

[28] R. Sareen and S. K. Gupta, *J. Appl. Polym. Sci.*, **58**, 2357 (1995).

[29] R. Sareen, N. K. Kohli, S. K. Gupta, *J. Appl. Polym. Sci.*, **62**, 1219 (1996).

[30] D.E.Goldberg and K.Deb, *A Comparative Analysis of Selection Schemes Used in Genetic Algorithm. Foundations of Genetic Algorithms*, Morgan Kaufman, San Mateo, CA, 1991, (pp. **69-93**).

[31] D. E. Goldberg and J. Rechardson, Genetic algorithms with sharing for multimodal function optimization. In J. J. Grefensetter (Ed.), *Genetic Algorithms and Their Applications: Proceedings of the Second International Conference on Genetic Algorithms* (pp. **41-49**). San Mateo, CA: Morgan Kaufmann (1987).

[32] R. Sareen, M. R. Kulkarni, and S. K. Gupta, *J. Appl. Polym. Sci.*, **57**, 209 (1995).

[33] K. Deb and D. E. Goldberg , *An Investigation of niches and species formation in genetic function optimization.* Proceedings of the Third International Conference on Genetic Algorithms, J. D. Schaffer (Ed.) (pp **42-50**).San Mateo, CA:Morgan Kaufman (1991).

[34] P. E. Gill, W. Murray, and M. H. Wright, *Practical Optimization*, Academic Press, New York, 1981.

Appendix 1

A1.1 Mass and Energy Balance Equations[12]:

$$\frac{d[C_1]}{dt} = -k_1[C_1][W] + k_1'[S_1] - k_3[C_1]\mu_0 + k_3'(\mu_0 - [S_1]) - R_{vm}/F \div [C_1]\frac{0.113R_{vm} + 0.018R_{vw}}{F}$$

$$\frac{d[S_1]}{dt} = k_1[C_1][W] - k_1'[S_1] - 2k_2[S_1]\mu_0 + 2k_2'[W](\mu_0 - [S_1]) - k_3[S_1][C_1] + k_3'[S_2] - k_5[S_1][C_2]$$

$$+k_5'[S_3] + [S_1]\frac{0.113R_{vm} + 0.018R_{vw}}{F}$$

$$\frac{d\mu_0}{dt} = k_1[C_1][W] - k_1'[S_1] - k_2\mu_0^2 + k_2'[W](\mu_1 - \mu_0) + k_4[W][C_2] - k_4'[S_2] + \mu_0\frac{0.113R_{vm} + 0.018R_{vw}}{F}$$

$$\frac{d\mu_1}{dt} = k_1[C_1][W] - k_1'[S_1] + k_3[C_1]\mu_0 - k_3'(\mu_0 - [S_1]) + 2k_5[C_2]\mu_0 - 2k_5'(\mu_0 - [S_1] - [S_2])$$

$$+2k_4[W][C_2] - 2k_4'[S_2] + \mu_1\frac{0.113R_{vm} + 0.018R_{vw}}{F}$$

$$\frac{d\mu_2}{dt} = k_1[C_1][W] - k_1'[S_1] + 2k_2\mu_1^2 + \frac{1}{3}k_2'[W](\mu_1 - \mu_3) + k_3[C_1](\mu_0 + 2\mu_1) + k_3'(\mu_0 - 2\mu_1 + [S_1])$$

$$+4k_5[C_2](\mu_0 + \mu_1) + 4k_5'(\mu_0 - \mu_1 + [S_2]) + 4k_4[W][C_2] - 4k_4'[S_2] + \mu_2\frac{0.113R_{vm} + 0.018R_{vw}}{F}$$

$$\frac{d[C_2]}{dt} = -k_4[C_2][W] + k_4'[S_2] - k_5[C_2]\mu_0 + k_5'(\mu_0 - [S_1] - [S_2]) \div [C_2]\frac{0.113R_{vm} + 0.018R_{vw}}{F}$$

$$\frac{d[W]}{dt} = -k_1[C_1][W] + k_1'[S_1] + k_2\mu_0^2 - k_2'[W](\mu_1 - \mu_0) - k_4[C_2][W] + k_4'[S_2]$$

$$-R_{vw}/F + [W]\frac{0.113R_{vm} + 0.118R_{vw}}{F}$$

$$\frac{dF}{dt} = -(0.113R_{vm} + 0.018R_{vw})$$

contd. A1b

$$\frac{dT}{dt} = \left\{UA\left(T_j - T\right) + \frac{F}{1000}\sum_{i=1}^{5} r_i\left(-\Delta H_i\right) - \left[R_{vm}\lambda_m\left(T_r\right) + R_{vw}\lambda_w\left(T_r\right)\right] - \left[0.113R_{vm}C^v_{p,m} + 0.018R_{vw}C^v_p\right.\right.$$

$$\left.\left.\times\left(T - T_r\right) + C^l_{p,mix}\left[0.113R_{vm} + 0.018R_{vw}\right]\left(T - T_r\right)\right\} \times \left\{\left[C^l_{p,mix} + 2.0925\times 10^{-3}\left(T - T_r\right)\right]F\right\}^{-1}\right.$$

$$\frac{d\left[M^v\right]}{dt} = \frac{R_{vm}}{V_g} - \frac{V_T\left[M^v\right]}{V_g\left(\left[M^v\right] + \left[W^v\right] + \left[N^v\right]\right)}$$

$$\frac{d\left[W^v\right]}{dt} = \frac{R_{vw}}{V_g} - \frac{V_T\left[W^v\right]}{V_g\left(\left[M^v\right] + \left[W^v\right] + \left[N^v\right]\right)}$$

$$\frac{d\left[N^v\right]}{dt} = -\frac{V_T\left[N^v\right]}{V_g\left(\left[M^v\right] + \left[W^v\right] + \left[N^v\right]\right)}$$

$$\frac{d\zeta_1}{dt} = R_{vm}$$

$$\frac{d\zeta_2}{dt} = R_{vw}$$

$$\frac{d\zeta_3}{dt} = V_T$$

Closure Conditions:

$$\left[S_3\right] = \left[S_2\right] = \left[S_1\right]$$

$$\mu_3 = \frac{\mu_2\left(2\mu_2\mu_0 - \mu_1^2\right)}{\mu_1\mu_0}$$

contd. A1c

A1.2 Correlations Used For Modelling[12]:

Expression for V_T

Stage 1: $V_T = 0$

Stages 2-5: $$V_T = R_{vm} + R_{vw} - \frac{V_g}{RT}\left(\frac{dP}{dt}\right) + V_g \frac{[M^v]+[W^v]+[N^v]}{T}\left(\frac{dT}{dt}\right)$$

Rates of vaporization

$$R_{vm} = F\left(k_{l,m}a\right)_f\left([C_l]-[C_l]_f^*\right) \qquad [C_l]_f^* = \frac{[W]+[C_l]}{\gamma_m P_m^{sat}}[M^v]RT$$

$$R_{vw} = F\left(k_{l,w}a\right)_f\left([W]-[W]_f^*\right) + F\left(k_{l,w}a\right)_b\left([W]-[W]_b^*\right)$$

$$[W]_f^* = \frac{[W]+[C_l]}{\gamma_w P_w^{sat}}[W^v]RT \qquad [W_b^*] = \frac{[C_l]\left(P-\gamma_m P_m^{sat}\right)}{\left(\gamma_w P_w^{sat}-P\right)}$$

Pressure

$$P = \{[M^v]+[W^v]+[N^v]\}RT$$

Equations for activity coefficients

$$\text{monomer conversion} = 1.0 - \frac{F[C_l]}{F_0[C_l]_0 - \zeta_1}$$

$$\gamma_m = \beta_{m0} + \frac{\beta_{mf} - \beta_{m0}}{0.95} \times (\text{monomer conversion})$$

$$\gamma_w = \beta_{w0} + \frac{\beta_{wf} - \beta_{w0}}{0.95} \times (\text{monomer conversion})$$

Vapor pressure

$$\ln\left[P_m^{sat}(kPa)/101.3\right] = 13.0063 - \frac{7024.023}{T(K)}$$

$$\ln\left[P_w^{sat}(kPa)/101.3\right] = 11.6703 - \frac{3816.44}{T(K) - 46.13}$$

Diffusion coefficients

$$\mathcal{D}_w\ (m^2\ h^{-1}) = 3.6 \times 10^{-6}$$

$$\mathcal{D}_m\ (m^2\ h^{-1}) = 2.88 \times 10^{-8}$$

contd. A1d

Latent heats of vaporization

$T_r = 473.15$ K

$\lambda_w(T_r) = 34.2559$ kJ mol^{-1}

$\lambda_m(T_r) = 51.0193$ kJ mol^{-1}

$C^v_{p,m} = 1.6426$ kJ kg^{-1} K^{-1}

$C^v_{p,w} = 1.9963$ kJ kg^{-1} K^{-1}

Heat transfer coefficient

$$h_i\ (\text{kJ h}^{-1}\ \text{m}^{-2}\ \text{K}^{-1}) = \frac{h_{ref}}{\left[\eta(\text{Pa\_sec})\right]^{0.17}}$$

$$U = \frac{1}{\frac{1}{h_i} + \frac{\text{thickness(m)}}{k_{SS}}}$$

Correlations for mixture physical properties (liquid)

$$C^l_{p,mix}\ (\text{kJ kg}^{-1}\ \text{K}^{-1}) = 2.0925 + 2.0925 \times 10^{-3}[T(K) - 273.15]$$

$$\rho\ (\text{kg m}^{-3}) = 1000\{1.1238 - 0.5663 \times 10^{-3}[T(K) - 273.15]\}$$

$$k\ (\text{kJ h}^{-1}\ \text{m}^{-1}\ \text{K}^{-1}) = 0.7558$$

Correlations for mass transfer coefficients

$$N_{Re} = \frac{d_s^2 n \rho}{6\eta(\text{poise})}$$

$$N_{Sc,l} = \frac{360\eta(\text{poise})}{\rho \mathcal{D}_i}$$

$$\Omega_b \equiv \left(\frac{[C_l]}{[C_l] + [W]} \gamma_m P_m^{sat} + \frac{[W]}{[C_l] + [W]} \gamma_w P_w^{sat} \right)$$

contd. Ale

(i) Quiescent (q) desorption ($\Omega_b < P$)

$$N_{Sh,i,q} = 0.322 N_{Re}^{0.7} N_{Sc,i}^{0.33}$$

$$N_{Sh,i,q} = \frac{\left(k_{l,i}\right)_{f,q} D_r}{\mathcal{D}_i}$$

$$a_{f,q} = \frac{(\pi/4) D_r^2}{(F/\rho)}$$

[*for* i = m or w]

$$\left(k_{l,m}a\right)_f = \left(k_{l,m}a\right)_{f,q}$$

$$\left(k_{l,w}a\right)_f = \left(k_{l,w}a\right)_{f,q}$$

$$\left(k_{l,w}a\right)_b = 0$$

(ii) Bubbly (b) desorption ($\Omega_b > P$)

$$\sigma \equiv \frac{[W] - [W_b]^*}{[W_b]^*}$$

$$\sigma_c \equiv 1.81 N_{Re}^{-0.25}$$

If $\sigma < \sigma_c$:

$$\left(k_{l,w}a\right)_b \left(h^{-1}\right) = 6.77 \times 10^{-6} N_{Re}^{0.5} \sigma^{0.78} \times 3600$$

$$\left(k_{l,m}a\right)_f = \left(k_{l,m}a\right)_{f,q}$$

$$\left(k_{l,w}a\right)_f = \left(k_{l,w}a\right)_{f,q}$$

If $\sigma > \sigma_c$:

$$\left(k_{l,w}a\right)_b \left(h^{-1}\right) = 2.45 \times 10^{-6} N_{Re}^{0.93} \sigma^{2.5} \times 3600$$

$$\log_{10}\phi \equiv 522(\sigma - \sigma_c) N_{Re}^{-0.81}$$

$$\left(k_{l,m}a\right)_f = \left(k_{l,m}a\right)_{f,q} \phi$$

$$\left(k_{l,w}a\right)_f = \left(k_{l,w}a\right)_{f,q} \phi$$

contd. A1f

Viscosity correlation (neglecting effect of water)

$$\eta_m(cp) = 2.7969 \times 10^{-1} \exp[3636.364/T(K)] \qquad \text{for } T > 473.15 \text{ K}$$

$$[\eta]\left(\frac{100 \text{ kg mixture}}{\text{kg polymer}}\right) \equiv \lim_{c\to 0}\frac{\eta_{sp}}{c} \equiv \lim_{c\to 0}\frac{\eta-\eta_m}{\eta_m}\frac{1}{c} = \left[-\frac{1875.0}{T(K)} + 4.678\right]\left(\frac{M_n}{5424}\right)^{0.75}$$

$$M_n = 113\mu_1/\mu_0$$

$$M_w = 113\mu_2/\mu_1$$

$$c(\text{kg polymer}/100 \text{ kg mixture}) = 11.3\mu_1$$

For $c < 21.0/[\eta]$

$$\frac{\eta_{sp}}{c[\eta]} = 1.0 - 0.3102c[\eta] + 0.0575(c[\eta])^2 - 0.525\times 10^{-2}(c[\eta])^3 + 0.2305\times 10^{-3}(c[\eta])^4 - 0.3663\times$$

For $c > 21.0/[\eta]$

$$\log_{10}\eta(\text{poise}) = 5\log_{10}\left(C_s' M_w^{0.68}\right) - 12.3097$$

for $C_s' M_w^{0.68} > 315$ and $M_w > 5000$

else

$$\log_{10}\eta(\text{poise}) = \log_{10}\left(C_s' M_w\right) - 3.503$$

where

$$C_s'(\text{gm polymer}/\text{cm}^3 \text{ mixture}) = 11.3\times 10^{-5}\rho\mu_1$$

CHE-1997-M-MIT. MUL